Theses and Dissertations--Medical Sciences   Medical Sciences

2022

Classification and Effect of Correctors on Sitosterolemia-Associated Mutants in ABCG8

Brittney Poole

University of Kentucky, brittney.poole@uky.com
Author ORCID Identifier:
http://orcid.org/0000-0002-0955-8815
Digital Object Identifier: https://doi.org/10.13023/etd.2022.339

Right click to open a feedback form in a new tab to let us know how this document benefits you.

Recommended Citation

CLASSIFCATION AND EFFECT OF CORRECTORS ON SITOSTEROLEMIA-
ASSOCIATED MUTANTS IN ABCG8

———————————————————————

THESIS

———————————————————————

A thesis submitted in partial fulfillment of the
requirements for the degree of Master of Science in the
College of Medicine
at the University of Kentucky

By

Brittney Poole

Lexington, Kentucky

Director: Dr. Gregory A. Graf, Professor of Pharmaceutical Sciences

Lexington, Kentucky

ABSTRACT OF THESIS

CLASSIFICATION AND EFFECT OF CORRECTORS ON SITOSTEROLEMIA-
ASSOCIATED CYTOSOLIC MUTANTS IN ABCG8

Objective: To classify mutants of ABCG8 identified in subjects with clinically confirmed Sitosterolemia, a rare form of Familial Hypercholesterolemia distinguished by the accumulation of phytosterols in plasma and tissues and determine the effects of correctors and/or regulators of proteostasis on maturation of the ABCG5/ABCG8 sterol transporter.

Methods: Disease-causing missense mutants within the cytosolic domain of ABCG8 were generated through site-directed mutagenesis. Normal and mutant proteins were expressed in human hepatocytes. Cellular proteins were prepared, and maturation was assessed by SDS-PAGE and immunoblotting. Formation of the higher molecular weight, mature form of glycoproteins was used as a bioassay for trafficking the G5G8 complex beyond the Endoplasmic Reticulum. The impact of correctors and regulators of proteostasis on Class II mutant maturation was also determined.

Results: Approximately 44% of cytosolic, Sitosterolemia-associated mutants in ABCG8 are maturation incompetent. Of those which matured beyond the ER, 60% were not able to traffic to the cell membrane. Of the mutants that did not mature, none were able to be rescued by small molecular chaperones (correctors).

Conclusion: HuH-7 cells are an efficiently transfected cell line that provides a system to manipulate ABCG5 and ABCG8 to make conclusions about protein maturation and trafficking to the cell surface. These experiments gave insight into the complexity of diseases caused by genetic mutations and the underlying mechanism of loss-of-function mutations. Further experimentation would be required to determine the fate of the CFTR correctors and/or regulators of proteostasis in the application in cases of Sitosterolemia.

KEYWORDS: Sitosterolemia, ABC transporters, lipids, correctors, proteostasis

Brittney Poole
(Name of Student)

07/27/22
Date

CLASSIFICATION AND EFFECT OF CORRECTORS ON SITOSTEROLEMIA-
ASSOCIATED CYTOSOLIC MUTANTS IN ABCG8

By

Brittney Poole

| Gregory A. Graf |
| Director of Thesis |

| Melinda Wilson |
| Director of Graduate Studies |

| 07/27/22 |
| Date |

ACKNOWLEDGMENTS

TABLE OF CONTENTS

LIST OF TABLES

LIST OF FIGURES

CHAPTER 1. INTRODUCTION

1.1 Background

Sitosterolemia is a rare form of familial hypercholesterolemia (FH) caused by two mutations in either the ATP-Binding Cassette protein (*ABC*) *G5* or *G8* gene, which is in close proximity of 375 bp between the initiation codons and share a common promotor that function in a head-to-head orientation [1,2,3]. Sitosterolemia results from a lack of function for ABCG5 or G8 in the absence of their respective binding partner, which is distinguished from other forms of FH. Sitosterolemia is an autosomal recessive inherited disease that affects about 1 in 200,000 individuals; however, it is unclear how often this disease is misdiagnosed. Clinical laboratory assays fail to distinguish cholesterol from phytosterols. Consequently, plasma from a patient with Sitosterolemia would present with what appears to be elevated total plasma cholesterol in clinical lab testing. Gas or liquid chromatography is required to distinguish phytosterols from cholesterol, a technique and instrumentation often unavailable in clinical laboratories.

Individuals diagnosed with FH and Sitosterolemia similarly present with xanthomas and premature coronary artery disease. The two diseases are distinguished by dominant vs. recessive genetics, clinical presentation, and sterol composition in the plasma. FH patients present with elevated LDL cholesterol, while Sitosterolemia patients present with increased plasma phytosterol, decreased excretion of phytosterols and cholesterol, and hemolytic and blood disorders [4,5]. The underlying genetic causes of FH and Sitosterolemia differ. In cases of FH, the mutations affect either *LDL-R*, its ligand Apolipoprotein B (*ApoB100*), or the machinery required for LDL/LDL-R internalization,

1

LDL Receptor Related Protein-Associated Protein 1 (LRPAP1) or proprotein convertase subtilisin/kexin type 9 (*PCKS9*) while Sitosterolemia results from genetic mutations in *ABCG5* and/or *ABCG8.*

Many ABC transporters are associated with diseases such as; Cystic Fibrosis (*ABCC7*), Progressive familial intrahepatic cholestasis type 3 (*ABCB4*), among others (Table 1.1)[6]. Investigation and FDA-approved drugs (Roscovitine; CFTR modulators) partially restore function to ABCC7 and ABCB4 mutants based on their underlying molecular defect. The rationale behind testing these modulators on cytosolic mutants of ABCG8 is that if these correctors and regulators of proteostasis are effective in multiple ABC transporters, then due to the evolutionarily conserved nature of the ABC transporters (Fig. 1.2-1), these may also be effective for mutants of ABCG8[7].

Table 1.1 ABC Transporters and their associated disease[46].

ABC Transporter	Associated Disease
ABCA1	Tangier's Disease/Familial Hypoapoproteinemia
ABCA4	Stargardt's Disease
ABCB2/3	Immune Deficiency
ABCB4	PFIC3
ABCB7	Anemia
ABCB11	PFIC2
ABCC2	Dubin-Johnson Syndrome
ABCC6	Pseudoxanthoma Elasticum
ABCC7	Cystic Fibrosis
ABCD1	X-linked Adrenoleukodystrophy (ALD)

Table 1.1 shows different ABC transporters and their associated diseases, demonstrating a wide range of diseases caused due to mutations in ABC transporters.

We hypothesize that small molecule correctors will enhance the maturation of native G5/G8 complex and Class II, maturation deficient mutants of ABCG8.

1.2 Cholesterol vs. Phytosterols

Sterols are an essential cellular component of eukaryotic membranes, with cholesterol in animal cells and phytosterols in plant cells. Cholesterol creates rigidity and curvature to the plasma membrane of animal cells. Cholesterol is acquired through diet or is generated by *de novo* synthesis. Cholesterol biosynthesis is a tightly regulated process that demonstrates negative feedback inhibition. When cholesterol is in excess, it can be toxic to the cell, while cells depleted of cholesterol cannot undergo normal physiological responses, for example, receptor signaling[8]. The transcription factor sterol regulatory element-binding protein 2 (SREBP2) regulates gene expression of the enzymes responsible for cholesterol biosynthesis and uptake to maintain homeostasis[9]. While endogenous cholesterol synthesis is tightly regulated, dietary cholesterol ranges due to dietary preferences and may be a pro-atherogenic factor[10].

Phytosterols are not endogenously synthesized *de novo* and are strictly enter from the diet. Phytosterols are structurally similar to cholesterol, but differ from cholesterol by the side chain on the D ring of the sterol backbone (Fig. 1). For this reason, chromatography and/or mass spectrophotometry is required to distinguish phytosterols from cholesterol in the plasma. Phytosterols have an observed toxicity in the body, as a study of ABCG5/ABCG8 KO mice fed a high-phytosterol showed signs of premature death, cardiac lesions, liver damage, and hepatosplenomegaly[11]. With a functional ABCG5/8 transporter effectively opposing absorption and excreting of phytosterols into the feces, mice and humans are not affected by high-phytosterol containing diets[11]. In a typical lipid panel used to measure cholesterol, cholesterol oxidase attacks the 3ß-hydroxyl group on the A ring of cholesterol. This structural feature is shared among sterols (animal/phytosterols) (Fig. 1)[12].

4

GC-Mass Spectrometry would be required to separate phytosterols from cholesterol in a plasma sample.

It has been proposed that phytosterols help reduce LDL cholesterol by competing with cholesterol for intestinal absorption resulting in a modest reduction (30-50%) of cholesterol absorption and a 10% decrease in total plasma cholesterol[13]. The mechanism by which phytosterols compete with cholesterol for intestinal absorption is by reducing the solubilization into the mixed micelle. However, other studies suggest phytosterols promote cholesterol secretion[13,14,15].

Figure 1.2-1 Cholesterol and Phytosterol structure.
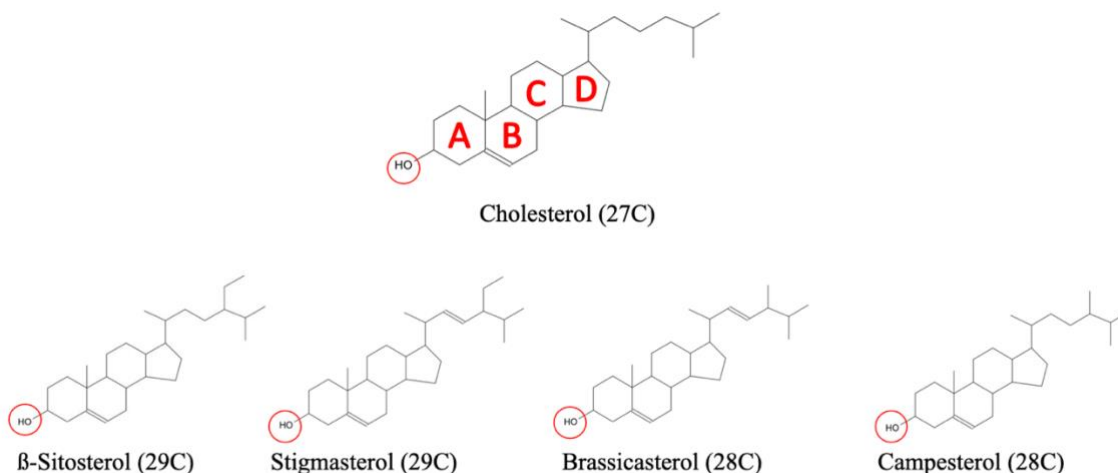
Figure 1.2-1 Chemical structure of cholesterol and 4 of the most common phytosterols showing the differences in side chains as well as the common 3ß-Hydroxyl group. The red circle indicates common 3ß-Hydroxyl amongst sterols and ring structures are labelled in cholesterol.

1.3 Sterol Absorption and Excretion

As previously mentioned, cholesterol can enter the body in one of two ways. Cholesterol-esters and phytosterols that enter the body exogenously are metabolized by enzymes (pancreatic lipases) and emulsified with bile salts and phospholipids that enter

the intestinal lumen via the gallbladder, ABCB11, and ABCB4, respectively, along with

dietary cholesterol to form mixed micelles. Mixed micelles act as the "cholesterol

acceptor" for dietary sterols[16]. Free cholesterol and phytosterols are absorbed from the

mixed micelle into the small intestine (duodenum/jejunum) by NPC1L1[17,18]. NPC1L1

(Niemann-Pick C1 Like 1) functions at the apical surface of enterocytes and mediates the

internalization of cholesterol and phytosterol to promote absorption[19]. In the enterocyte,

cholesterol is esterified by the enzyme ACAT-2 (Acyl-CoA: Cholesterol

Acyltransferase), which preferentially esterifies cholesterol relative to phytosterols[20].

Cholesterol is incorporated into chylomicrons, secreted into the lymphatic system, and

enters the plasma compartment via the left subclavian vein. Cholesterol and plant sterols

that are not esterified by ACAT are exported by ABCG5/G8 back to the intestinal lumen.

In the plasma compartment, chylomicrons and triglycerides are metabolized by

Lipoprotein lipases (LPL), generating a smaller, cholesterol-rich chylomicron remnant,

which can enter the liver via LDL-R or other related receptors. This pathway delivers

dietary cholesterol and re-absorbed biliary cholesterol to the liver.

Another mechanism by which cholesterol can enter the liver is reverse cholesterol

transport (RCT). RCT is a pathway in which cholesterol accumulated in peripheral tissue

is transported through the plasma to the liver for excretion as neutral sterols or bile acids

in the feces[21]. Peripheral tissues, such as macrophages, export excess cholesterol by

ABCA1 to a pre-HDL particle composed of a lipidated Apo-A1. This process is

dependent on the Lecithin Cholesterol Acyltransferase (LCAT) enzyme. LCAT esterifies

cholesterol to fatty acids to generate cholesterol esters that get deposited in the core of

HDL particles[22]. As opposed to ACAT, LCAT is thought to freely esterify phytosterols to

generate mature, spherical HDL. ABCG1, SR-B1, CD36, and other possible sterol transporting enzymes can deliver esterified sterols in the form of HDL to the liver through Scavenger Receptor Class B I (SR-BI)[23].

Once cholesterol enters the hepatocyte, it can be excreted in one of two ways. The first pathway is metabolism by cytochrome P450 enzymes (ex. CYP7A1/CYP27A1) into bile salts. Bile salts are secreted at the canalicular membrane of hepatocytes by the transporter BSEP (Bile salt export protein, ABCB11)[23]. The other mechanism by which cholesterol can be excreted from the liver is as free cholesterol via ABCG5/8, which also functions at the hepatocyte canalicular membrane. However, 95% of bile acids and 80% of cholesterol secreted will be re-absorbed in the intestine by apical sodium bile acid transporter (ASBT) and Niemann-Pick C1-Like 1 (NPC1L1)[25,26] . Alternatively, sterols can return to the plasma in the form of VLDL particles along with Apo-B100, triglycerides, and LDL particles are secreted from the liver a shared mechanism with chylomicrons and ultimately give rise to the LDL particle. Both chylomicron remnants and LDL are pro-atherogenic particles.

The Transintestinal Cholesterol Excretion (TICE) pathway is an alternative pathway to hepatobiliary excretion of cholesterol from the body. TICE is the process of cholesterol transport from the bloodstream, across the enterocyte, and directly into the intestinal lumen[27]. Cholesterol is taken up by LDL-R on the basolateral membrane of enterocytes (with possibilities for another pathway)[28]. Cholesterol is then translocated across the enterocyte and secreted via ABCG5/8 at the apical membrane for excretion in the feces or possible reabsorption by NPC1L1[28]. This alternate pathway is thought to account for 30-50% of RCT[29].

1.4 Sitosterolemia

In 1974, two sisters presented with tuberous xanthomas and plasma plant sterols that accounted for roughly 30% of their total plasma sterols. In a typical human subject, plant sterols are typically only detected in trace amounts due to poor absorption, only about 5%[4]. Both parents of the sisters that unaffected, leading to the conclusion that this rare lipid disease was inherited in an autosomal recessive manner[4]. It wasn't until 2000 that *ABCG5* and *ABCG8* were discovered to be the two genes mutated in clinically confirmed patients with Sitosterolemia[30]. In 2003, it was confirmed that ABCG5 and ABCG8 function as obligate heterodimers, with both proteins being required to reach the cell surface and transport sterols across the membrane[31]. In addition to the previously reported phenotypes of Sitosterolemic patients, subjects with clinically confirmed Sitosterolemia could also present with hematological abnormalities, including macrothrombocytopenia, hemolytic anemia, and splenomegaly[5].

Currently, the primary treatment(s) for Sitosterolemic patients are dietary modifications (low sterol diet), Ezetimibe, bile acid-binding resins, ileal bypass surgery, or LDL apheresis. However, these treatments decrease plasma phytosterols and improve symptoms but fail to return plasma sterols to the range of a normal human subject[32]. Ezetimibe is an NPC1L1 inhibitor, reduces cholesterol, and phytosterol absorption by ~50%, and is currently the primary pharmacotherapy used to treat cases of Sitosterolemia[33]. While Ezetimibe has shown efficacy in reducing phytosterol accumulation, the drug does not target ABCG5/G8. This is important because ABCG5/8 promotes sterol, primarily phytosterol, efflux at the enterocyte and hepatocyte apical surface, whereas NPC1L1 primarily functions in sterol absorption in the enterocyte.

NPC1L1 is highly expressed in both the liver and intestine and oppose biliary sterol secretion in humans, while there is low expression in mice liver[19]. Even if phytosterol uptake into absorption is opposed, there is still a lack of hepatic secretion and an inability to eliminate phytosterols from plasma and tissues once accumulated (Fig. 1.4-1).

Figure 1.4-1 Diagram demonstrating the absorption, excretion, and secretion pathway of phytosterols and current therapeutics for Sitosterolemia.
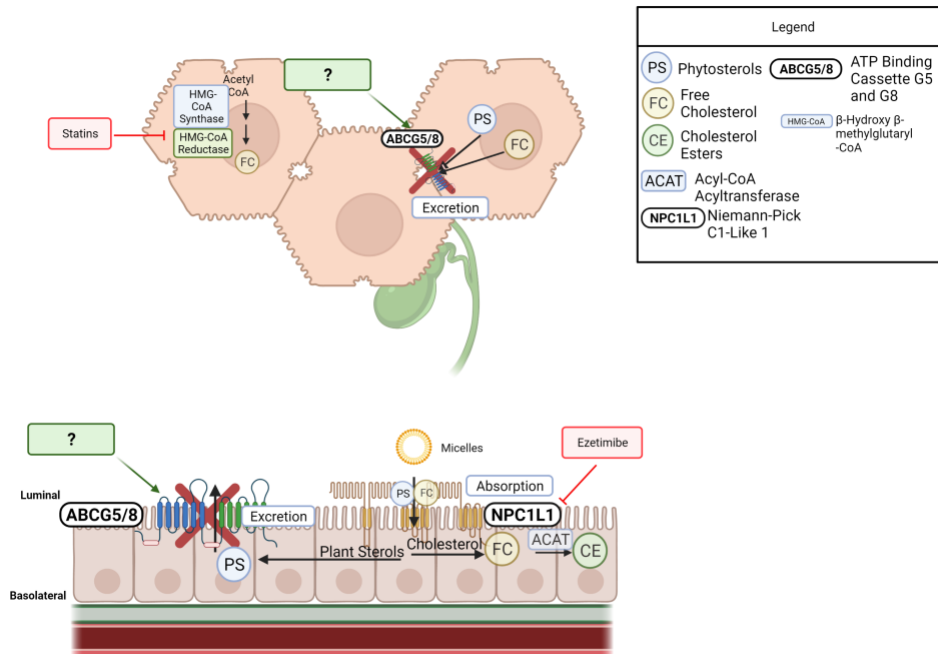
Figure 1.4-1 Pathway for excretion and secretion of phytosterols in the liver and intestine. Diagram also exhibits the mechanism of action for ezetimibe, the most common current treatment management of Sitosterolemia.

In a 10-year follow-up study of two sisters who had a homozygous nonsense mutation (R446X in *ABCG5*), treatment with Ezetimibe only moderately decreased phytosterol levels while diet changes had little to no change on phytosterol levels[34]. Starting phytosterol (sitosterol and campesterol) levels were greater than 300 µmol/L and decreased to ~100 µmol/L, however, the normal range for a healthy individual is 10-20 µmol/L[34]. While Ezetimibe is a form of Sitosterolemia management, these patients still have far higher cholesterol and phytosterol absorption, which can increase the risk of

cardiovascular events later in life. This demonstrates a need for a more specific pharmacologic agent that targets the underlying molecular defect of ABCG5 and ABCG8 disease-causing mutants as opposed to disease management through Ezetimibe.

1.5 ABCG5/G8 Physiology

ABCG5 and ABCG8 (ABCG5/8) are two ABC-half transporters that function as a heterodimer at the apical membrane of hepatocytes (liver) and enterocytes (small intestine)[30]. *ABCG5* and *ABCG8* at the transcriptional level have been shown to be regulated by two nuclear receptors, Liver X Receptors (LXR) and Farnesoid X Receptors (FXR). LXRα and β belong to the family of nuclear receptors that are master regulators of genes involved in cholesterol elimination pathways and form heterodimers with Retinoid X Receptors (RXR)[35]. These transcriptional factors are activated by cholesterol metabolites, oxysterols[36]. It was determined that gene expression of *ABCG5* and *ABCG8* was increased when mice were fed a high cholesterol diet in wildtype mice but in LXR$^{-/-}$, indicating the two genes are also regulated by the LXR/RXR transcription factor[37]. *ABCG5* and *ABCG8* can also be upregulated by the FXR pathway, a nuclear receptor activated in the presence of bile acids[37]. *ABCG5* and *ABCG8* are also positively regulated by the transcription factors hepatocyte nuclear factor 4α (HNF4α), Forkhead box protein O1 (FOXO1), and Liver receptor homolog 1 (LRH1), but the relationships to sterol homeostasis are not as clear[38,39].

Beyond the nucleus, ABCG5 and ABCG8 are independently translated in the rough ER. It is unclear how ABCG5 and ABCG8 emerge from the ribosome and find their respective binding partner. Within the ER, ABCG5 and ABCG8 are recognized by

molecular chaperones, such as calnexin, that facilitate folding of the ABCG5/ABCG8 complex in an N-linked glycan-dependent mechanism. Chaperones recognize the terminal glucose on the N-linked glycan, a tag that sorts proteins for their destination. Proteins that are unfolded are recognized by a glucosyltransferase in the ER and the protein is either is re-glucosylated or exits the chaperone folding "cycle." If in fact ABCG5/8 have dimerized, they are sorted to the apical membrane through the cell's secretory pathways to function as a heterodimer[40].

In summary, ABCG5/G8 function as an obligate heterodimer at the apical surface of hepatocytes and enterocytes. In the liver, ABCG5/8 promotes secretion of phytosterols and cholesterol into bile[31]. In the intestine, ABCG5/G8 opposes phytosterol absorption by NPC1L1. In mice, expression in one organ, either liver or intestine, is sufficient to protect the animal from Sitosterolemia and the downstream effects of phytosterol accumulation[41]. However, it is unclear whether this remains true regarding RCT.

1.6 ABC Transporters

ABC transporters are a family of integral proteins that function to translocate substrates across membranes, a mechanism powered by ATP hydrolysis[7]. The ABC transporter superfamily consists of 48 proteins and can be further divided into subfamilies, A-G[42]. The key characteristics of ABC transporters are two nucleotide-binding domains (NBD), two transmembrane domains (TMD) that have 12 membrane-spanning alpha-helices, and two ATP-Binding Cassette's (ABC), however, there are exceptions among the ABC transporters (Fig. 2)[42,43]. Among the 48 transporters in humans, there are half transporters (ABCG5/8) and full transporters (for example,

ABCB1). The NBD of ABC transporters is a domain that is highly conserved and includes the Walker A motif, Walker B motif, Walker C motif (signature motif), Q-loop, and H-loop (switch motif)[6,7].

While structurally similar across ABC transporters, the TMD sequence differs significantly across and within families, likely a reflection of different substrate binding pockets[6]. The NBD binds and hydrolyzes ATP to power the pump[6]. ATP binds to both of the NBDs which forms a tight dimer and two ATPase active sites[44]. A helix in the TMD fits into a groove on the NBD, resulting in the opening and closing of the NBD simultaneously to transmembrane helices movement[44].

Figure 1.6-1 Structure of ABC transporter families[45].
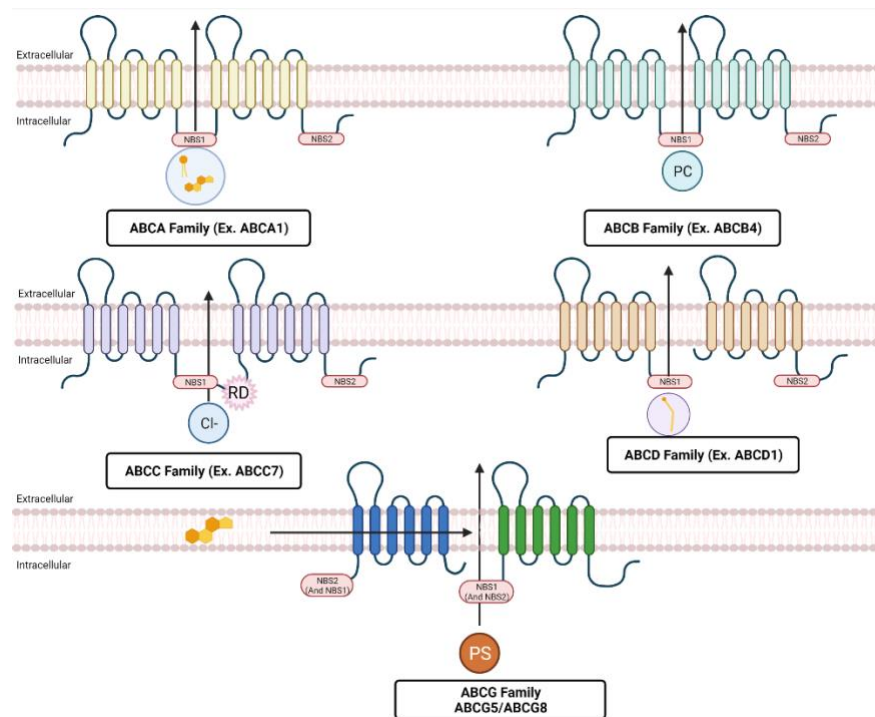
Figure 1.6-1 Structure of the ABC transporter families showing the Transmembrane domain and Nucleotide Binding domain, as well as the structural differences between each of the families, most notably differences in whether the NBD resides at the N or C-terminus.

ABC Transporters import (prokaryotes) or export (eukaryotes) substrates via ATP hydrolysis cycling[7]. Substrate translocation begins with the substrate binding to the TMD and initiating a conformational change from an open to closed conformation. After the substrate is bound to the TMD, ATP can bind to the NBD, which induces the ATP "power stroke" and promotes the closed formation of the TMD. ATP is then hydrolyzed into ADP and inorganic phosphate (Pi), effectively translocating the substrate. The release of ADP and Pi indicates the end of the ATP hydrolysis cycle. The protein is restored to its original open conformation and is ready to transport another substrate across the membrane[6].

The G family of ABC transporters all function as dimers and transport sterols[47]. Sterols, and a number of other lipids, are amphipathic and insoluble in water. Sterols require carriers and transporters to move through the body and plasma membrane. ABCG1, 2, and 4 are functionally active as homodimers while ABCG5/G8 is functionally active as an obligate heterodimer. ABCG1/4 have been proposed as candidates for heterodimerization due to their sequence similarity, although the evidence is lacking[48]. ABCG5/8 specifically functions to secrete sterols from hepatocytes into bile and from enterocytes back to the intestinal lumen for excretion. Both hepatocytes and enterocytes are polarized cell types each expressing an apical and basolateral membrane that serve different functions for the cell in addition to different transporter makeup. NBS2 is thought to be the driver of conformational change with respect to ATP hydrolysis and sterol transport while NBS1 binds ATP but does not hydrolyze it[49]. NBS1 and NBS2 are located within ABCG5 and ABCG8[49].

Many ABC transporters that are disease-causing, such as ABCC7/Cystic Fibrosis or ABCB4/PFIC3, have systems to classify mutations[50,51]. Shown in Table 1.2 is the proposed classification system for Sitosterolemia-associated G5/G8 mutations based on the systems mentioned above already in place[52]. Class I mutants are nonsense/frameshift/deletion mutations, whereas classes II-V are missense mutations. Class II mutants are defective in maturing beyond the Endoplasmic Reticulum, class III mutants are ones in which the protein is properly folded but lack functional activity, class IV mutants are unstable, and class V mutants are proposed to be defective in trafficking at the apical surface.

Table 1.2. Proposed Sitosterolemia Classification System[52]

CLASS	DESCRIPTION	ABCG5 MUTANTS	ABCG8 MUTANTS
I	Nonsense, Frameshift, Deletion	57 known or predicted	58 known or predicted
II	Maturation	R389H, R419P, N437K	R189H, P231T, R236Q
III	Activity		
IV	Stability		
V	Trafficking		
Unclassified	Inconclusive Results	E146Q	R543S

Table 1.2. Table of proposed Sitosterolemia classification system in addition to previously published classifications of ABCG5 and G8 mutants.

1.7 Proteostasis Regulation and Roscovitine

Proteostasis (protein homeostasis) refers to the process of maintaining a protein's quaternary structure and location, typically through transcriptional/translational modifications[53]. Proteostasis influences protein synthesis, folding, trafficking, disaggregation, and degradation[53]. The ER is responsible for the synthesis, folding, maturation, and trafficking of transmembrane proteins as well as secretory proteins. In disease states where proteins are misfolded, proteostasis pathways detect and rapidly degrade the misfolded proteins via the Endoplasmic Reticulum-Associated Degradation (ERAD) pathway. Disruptions in protein folding trigger of ER Stress and activate the Unfolded Protein Response (UPR). Conditions that disrupt protein homeostasis and activate UPR are changes in temperature, calcium concentration disturbance, mutations, redox disruptions, and changes in cellular pH[54].

The unfolded protein response (UPR) is activated when the cell's protein folding machinery becomes overwhelmed and misfolded proteins accumulate in the ER[55]. Disruption of protein homeostasis occurs in conditions as previously mentioned, including mutant proteins, alterations in gene expression, or permanently when there are mutations that affect protein maturation[56]. The ERAD (ER-Associated Degradation) pathway is an essential step in newly synthesized protein quality control[57]. Chaperones recognize proteins such as calnexin/calreticulin and heat-shock proteins, which facilitate folding. Transmembrane proteins are glycosylated with an N-linked glycan and the terminal glucose acts a tag that the protein is unfolded and thus recognized by calnexin/calreticulin. Proteins that are unfolded are recognized by a glucosyltransferase in the ER and the protein is either re-glucosylated or exits the chaperon folding "cycle." When prolonged, the misfolded protein is targeted by the retro-translocon and/or E3 ligases[58]. The misfolded protein is then retrotranslocated to the cytoplasm, ubiquitinated by E3 ligases, recognized by the 19S cap of the 26S proteasome, and degraded[58].

Roscovitine is a small molecule pharmacologic that arrests cell cycle progression by inhibiting cyclin-dependent kinases (CDK) 1, 2, 5, 7, and 9[59]. Roscovitine was first studied in ABC transporters in its rescue of an ABCC7 (CFTR) mutant, F508del[60]. The group suggested that the mechanism of action of Roscovitine F508del correction was likely independent of inhibition of CDK's and, more generally in inhibition of kinases as well as directly inhibiting activity of the proteasome[60]. This led to the proposal of Roscovtine's rescue of F508del through modulation of proteostasis, specifically the ERQC (ER quality control) and ERAD system independently[60]. The research done by this group influenced another group (Falguières) to test Roscovitine on three ABCB4

16

mutants in an attempt to achieve similar outcomes[61]. The three mutants tested were class II (maturation deficient) mutations[61]. Because ATP transporters are well conserved across ABC transporter families, there are potential compounds successfully used in other ABC transporter families that could be repurposed to treat Sitosterolemia-associated ABCG8 mutations.

Mutations in class II that get retained in the ER would make a compound like Roscovitine a viable target for "rescuing" defective ABCG5/G8 transporters, as it has shown the ability to modulate proteostasis[60]. It has been well established that ABCG5/G8 are poor folding proteins, as only about 40-50% of the protein matures beyond the ER, which strengthens the argument for potential stabilization[31]. Roscovitine has significant cellular toxicity. Therefore, 11 analogs were synthesized in an attempt to lower CDK inhibition and cytotoxic activity (Table 1.3)[61]. Some of these analogs partially rescue mutants of ABCB4, which strengthens the hypothesis that Roscovitine rescue works independently of CDK inhibition in ABCC7 and ABCB4. The efficacy of Roscovitine across multiple ABC transporters (ABCB4/ABCC7) and their structural similarities to ABCG5/G8 is the scientific premise of this project.

Table 1.3. Roscovitine and Analogs Structure.
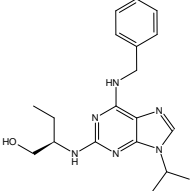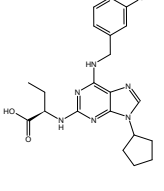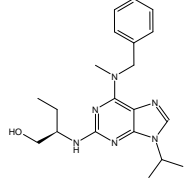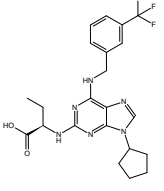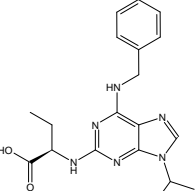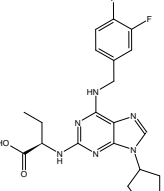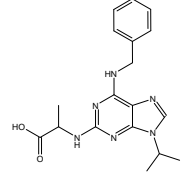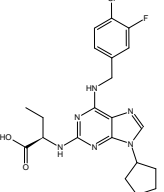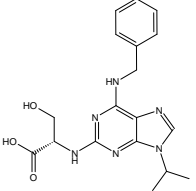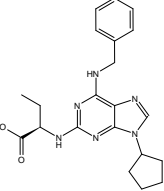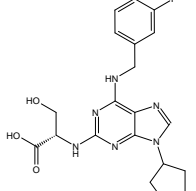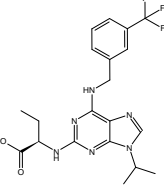
Compound Name	Compound Structure	Compound Name	Compound Structure
Roscovitine		MRT2-237	
Aftin-4		MRT2-239	
M3		MRT2-241	
MRT2-163		MRT2-243	
MRT2-164		MRT2-245	
MRT2-235		MRT2-249	

Table 1.3. Table of Roscovitine and 11 analogs synthesized by ManRos Therapeutics[61].

1.8 Ivacaftor and ABCC7 Potentiation

Cystic Fibrosis (CF) is a disease in which the Cystic Fibrosis Transmembrane

Regulator (CFTR), *ABCC7*, fails to flux chloride ions leading to an accumulation of

chloride ions in the epithelial cells and in turn a change in mucus viscosity in the

lungs[62,63]. Ivacaftor is an FDA-approved Cystic Fibrosis treatment that potentiates

(increased channel open probability) CFTR and partially restores chloride ion transport.

ABCC7 differs from most ABC transporters as it is an ion channel that utilizes ATP

hydrolysis, whereas ABCG5/8 is a protein transporter that uses energy from ATP to

efflux sterols[64]. Ivacaftor potentiator function in CFTR has therapeutic benefits in

patients with CFTR gating (class III) defective mutations[50,65]. The mechanism of action

of Ivacaftor is binding to the PKA-phosphorylated ABCC7 in an ATP-independent

fashion[66]. Ivacaftor functions mainly for mutations that disrupt gating due to disruption to

the ATP-dependent binding site[66]. It has not been reported that regulation of ABCG5 and

ABCG8 is PKA-dependent and ABCG5/G8 does not operate as an ion channel.

Therefore, there is not a strong foundation for why Ivacaftor would be able to stabilize

mutants of ABCG8.

However, in maturation, defective mutants of CFTR are "rescued" by small

molecule correctors of the Ivacaftor-family (Table 1.4), which may facilitate folding of

ABCG5/G8. Elexacaftor, Tezacaftor, and Lumacaftor are compounds that were

formulated after Ivacaftor for CF mutants that were not gating defective. They are small

molecular "correctors" as they correct the misfolding of proteins that fail to exit the ER.

The correctors' mechanism of action is directly binding to CFTR, but how they function

as a protein folding chaperone to escape degradation remains unclear. Rescued CFTR

mutants localize to the cell surface[67]. This suggests that escaping ERAD is sufficient for activity. In more recent studies, looking at the cryo-EM structure of CFTR in complex with Lumacaftor or Tezacaftor demonstrates that the drugs bind to CFTR in the hydrophobic pocket of TMD-1, which ultimately stabilized the domain and prevented degradation[68]. Lumacaftor and Tezacaftor bind within the hydrophobic pocket at a Lysine and Arginine residue before the start of the TMD-1[68]. ABCG5 is structurally similar in that it too has a Lysine and Arginine residue prior to the start of the first TM domain[49]. One could hypothesize that because of this structural similarity there is potential for Lumacaftor or Tezacaftor binding to ABCG5 at the apical membrane.

There is a much larger family of CFTR modulators (including correctors) that are being investigated *in vitro* that have demonstrated stabilization in mutants of multiple ABC transporter systems. Most notably, correction of ABCG2 mutants involved in Gout by Cor-4a and due to sequence homology may too be effective in stabilizing Sitosterolemia-associated mutants[69]. Stabilization with these and other compounds could give reason to believe that these compounds could be used in Class II mutants across a wide range of ABC transporter-related diseases.

Table 1.4. Ivacaftor and Correctors Structure
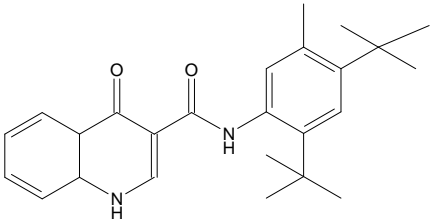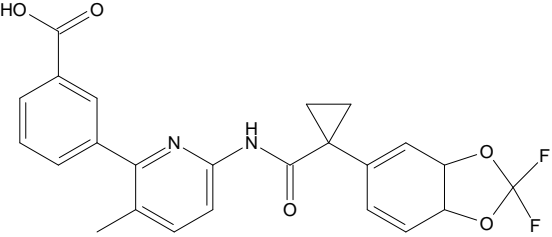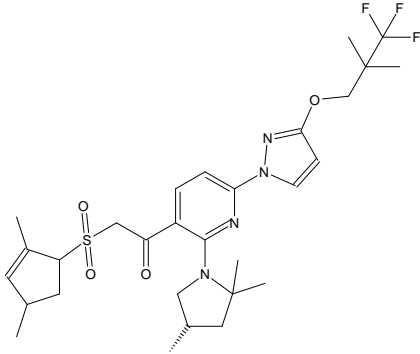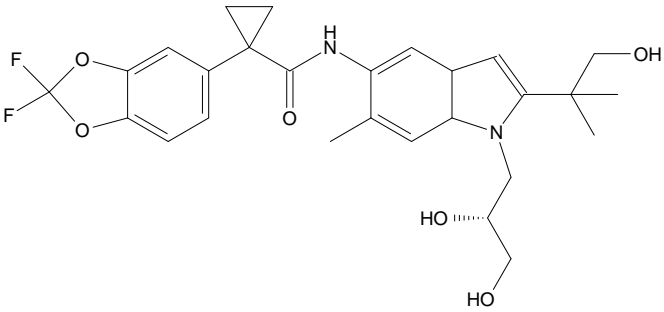
Compound Name	Compound Structure
Ivacaftor	
Lumacaftor	
Elexacaftor	
Tezacaftor	

Table 1.4: Chemical structures of Ivacaftor and CFTR correctors. Compounds were purchased from Medchemexpress or Selleckchem.

1.9 Statement of Hypothesis

This thesis aims to characterize Sitosterolemia-associated cytosolic mutants in ABCG8 based on their underlying molecular defects. The impact of correctors on maturation deficient mutants (class II) were tested for efficacy in correcting protein maturation in other ABC transporter families. For maturation competent mutants, we analyzed via immunofluorescence microscopy the degree to which mutants traffic to the plasma membrane. Maturation of ABCG8 Sitosterolemia-associated mutants and the effect of correctors will be studied *in vitro*, in a human hepatocyte carcinoma cell line.

We hypothesize that when transiently expressed in human hepatocytes, some ABCG8 missense mutations compromise protein folding, transporter complex formation, and trafficking beyond the Golgi. The addition of a compound with proteostatic regulator or CFTR corrector activity used to treat diseases caused by other ABC transporters may correct folding defects in ABCG8 caused by class II missense mutations.

CHAPTER 2. MATERIALS AND METHODS

2.1 Materials and Methods

2.1.1   Reagents

Roscovitine and its 11 analogs were generously sent to us by Laurent Meijer (ManRos Therapeutics). The CFTR modulators were ordered through Medchemexpress or SelleckChem (Elexacaftor). Dr. Mahmood Hussian (NYU Langone), provided the HuH-7 cells to test in our experiments. Antibodies used in our Western blotting and Immunofluorescent protocol include 1B10A5 Mouse anti-ABCG8 (Novus), in-house mouse anti-human ABCG8 hybridoma notated as KWE5, Rabbit anti-c-Myc (Upstate cell Signaling Solutions 06-549), Mouse anti-βactin (Sigma A5441-100UL), Rabbit anti-Calnexin (Enzo Lifesciences ADI-SPA-860-F), and E-Cadherin (Cell Signaling). For the LDH Assay, the Cytoscan LDH Cytotoxicity assay kit (G-Biosciences 786-324) was utilized to measure cytotoxicity.

2.1.2   Cell Culture

HepG2 and HuH-7 cells were grown and cultured in Dulbecco's Modified Eagle Medium (DMEM)-High Glucose supplemented with 10% FBS, 1% Pen-Strep, and 1% GlutaMax. HEK293 cells were grown and cultured in DMEM- High Glucose (Dulbecco's Modified Eagle Medium) supplemented with 5% FBS, 1% Pen-Strep, and 1% GlutaMax. All cell lines were incubated at 37°C and 5% CO_2.

2.1.3 GFP Assay

GFP Lysates were made by washing the cells with 2x PBS and incubating the cells in GFP Lysis Buffer (25 mM Tris (pH=7.8), 2mM trans-1,2-diaminocyclohexane-N'N'N'N'-tetraacetic acid, 1% Triton X-100, 10% Glycerol) for 30 minutes at 37°C and then 30 minutes at room temperature. The lysates were then imaged on a plate reader for fluorescence (excitation 485 nm/emission 515 nm) and absorbance of (280 nm) and expressed as fluorescence 515/280 (arbitrary units).

2.1.4 Western Botting Analysis

Cell lysates were analyzed for protein concentration with a Bicinchoninic acid (BCA) assay incubated at 37°C for 30 minutes and measured at an absorbance of 562 nm. Protein concentration was determined by a bovine serum albumin (BSA) standard curve in each assay. Samples were prepared in 5X Laemelli Buffer (Tris Base (250 mM, pH 6.8), SDS (2.5%), glycerol (50%), and bromophenol blue (0.125%)) and equal protein (15-25 ug) were loaded onto a 4-8% bis-acryl and ran at 100 V for approximately 2-3 hours to ensure the differences in immature/mature protein glycosylation were present. The gels were then transferred to a nitrocellulose membrane at 100 V at 4°C for 1 hour or using BioRad's semi-dry Turboblot system.

2.1.5   In-vitro Bioassay

Monitoring the shift in electrophoretic mobility on an SDS-PAGE gel is indicative of modifications to the N-linked glycan residue(s) attached in the third extracellular loop of either ABCG5 or 8. We used this change in apparent molecular weight in immunoblotting for ABCG5 or G8 as a marker for maturation. We quantified these measures by densitometric analysis and expressed the data as a percent (mature signal over total signal), an index (mature signal over immature signal), or total mature signal to loading control.

2.1.6   Densitometric Analysis

Gel files were analyzed for densitometry using Adobe Photoshop. Once the gel image was cropped, aligned, and at desired contrast, the gel image was uploaded into Photoshop and a duplicate image was created. The duplicate image was inverted and using the measurement tool, captured the integrated density for each band in the blot (mature band, immature band, and loading control) along with a background measurement. For each signal, the measurement size kept constant. The background was subtracted from each value and expressed as described for each experiment.

2.1.7 Immunofluorescence Microscopy

HuH-7 cells were seeded in a 10 cm dish with 6 UV-sterilized coverslips at ~1×10^6 cells. On day one, coverslips were transferred to a 6 well dish, and transfected with wildtype hG5-myc and either wildtype hG8 or mutant hG8. On day two, cells were fixed with Methanol by an adaptation of Ann Hubbards "Cassio" protocol. Cells were incubated with a primary antibody and a secondary conjugated fluorophore with either a 488 or 568 Alexa-Fluor tag. Coverslips were mounted with Molecular Probes ProLong Gold Antifade Mountant with DAPI mounting medium from ThermoFisher. This assay was done with or without treatment with 50 ug/ml cycloheximide to deplete the ER of new protein translation.

Cells were imaged with the Zeiss Axiovert 200M at the 100X objective as either still images or using confocal imaging using the Apotome camera. Each image was taken with about 10-12 slices, each at .3 um thick. The images were then processed using Axiovision as a 3D rendered image or z-stack slices.

2.1.8 Statistical Analysis

All cell culture experiments were analyzed by a one-way ANOVA with either a Tukey or Dunnett's post-hoc test (indicated within each experiment). Experiments with statistical analysis were repeated in triplicate giving an n=3, for most experiments. Statistical significance was expressed as follows; * $p<.05$, ** $p<.01$, *** $p<.001$, ****$p<.0001$.

2.2 Experiment I- Generation of Sitosterolemia Associated ABCG8 Cytosolic Mutants

Purpose: To generate ABCG8 Cytosolic Sitosterolemia-associated mutations to characterize each mutation based on its molecular defect. Mutation Database: A mutation database was generated to determine which mutations were "clinically" associated with Sitosterolemia. The database consisted of mutations that were clinically published from human subjects, predicted through the global minor allele frequency (GMAF), or likelihood of pathogenicity on the America College of Medical Genetics and Genomics (ACMG) scale. Two criteria were taken into consideration when determining which mutants would be analyzed. One, they had to be Sitosterolemia-Associated, either a published mutation in a clinically confirmed Sitosterolemia patient or high on the ACMG scale. Two, we only analyzed missense mutations. While several nonsense and frameshift mutations are associated with Sitosterolemia, we limited our studies to missense mutations. Truncated proteins, while have been described to be inactive proteins, were not in our analysis because one, they are already characterized as a class I mutant and two, there is little to no chance to "rescue" or stabilize a truncated protein with the modulators.

Experimental Design: ABCG8 mutants were generated via Site-Directed Mutagenesis. The workflow of each mutant is as follows: primer design, PCR reaction, DpnI Digest, Bacterial Transformation, SalI Digest, Gel Electrophoresis, and DNA Sequencing. In the primer design, oligos were designed using IDT and GeneArt software's to generate an oligo that was approximately 35-39 nucleotides long. The forward and reverse primers were designed as direct complements of each other, with the point mutation of interest directly in the middle of the oligo. The oligos were then reconstituted in TE Buffer at 100 μM.

The PCR reaction was designed according to the Pfu polymerase manufacturer's protocol and the annealing step temperature was based on the oligo melting temperature (Annealing temp= Tm - 5°C). DpnI is a restriction enzyme that cleaves methylated DNA produced by host cell machinery. Therefore, prior to the PCR reaction, the parent ABCG8 plasmid was methylated to ensure DpnI digest provided the proper negative control. Control reactions contained no Pfu polymerase and primers from one mutant. Changes to the Pfu manufacture protocol were: 18 total cycles and a 10minute extension time. Following PCR, the DNA was cleaned up using Qiagen Spin Miniprep 2.0 kit to remove buffers or salts. The DNA then underwent DpnI digest based on NewEngland Biolabs protocol and another round of DNA clean-up. After the second DNA clean-up, the DNA was transformed into DH5α competent cells and grown on Agar + 50 ug/ml Ampicillin plates. Bacterial colonies were then grown in LB Broth with 50 µg/ml of Ampicillin overnight at 37°C and 200 rpm. The colonies were prepped using the Qiagen Mini Prep kit and quantified using a Nanodrop spectrophotometer. If the colonies had a positive yield above 160 ng/µl, they were SalI digested based on NewEngland Biolabs protocol and ran on a 1% agarose gel, then fluorescently imaged using SYBR-Safe.

After confirmation that SalI cut the mutant plasmids at the equivalent cut sites to the parent ABCG8 plasmid, the plasmid was subjected to Sanger sequencing (Eurofins, Chicago, IL). The DNA sequence was then analyzed in SnapGene 4.3.11 to confirm desired base pair change. Once the desired base change was confirmed, the construct was sent for full plasmid sequencing of the coding region to check for any additional undesired mutations.

Figure 2.2-1 Example of Site-directed Mutagensis Restriction Enzyme Digest and sequence verification (Generated using Snapgene software version 4.3.11).

Fig. 2.2-1. A. Native ABCG8 and ABCG8 mutants were digested with the SalI restriction enzyme. The samples were then ran on a 1% Agarose gel and fluorescently imaged via SYBRsafe. B. Samples were Sanger sequenced (by Eurofins) and the output was importing to Snapgene 4.3.11. Parent hG8 native DNA compared to mutant DNA, showing a single base pair change resulting in a mutation of Leucine to Proline at amino acid position 228.

Table 2.5. Sitosterolemia-Associated Mutants generated by Site-Directed Mutagenesis in the Cytosolic Domain of ABCG8

Mutant	**Mutant**
R184H	T400K
L195Q	N409I
L228P	N409D
P231T	P415H
R263Q	

Table 2.5: Table of the nine cytosolic mutants in ABCG8 generated via site-directed mutagenesis

2.3 Experiment II- Optimization of Transient Transfection of Human Cell Lines

Purpose: ABCG5/8 are located on the apical membrane of hepatocytes and enterocytes, both showing difficulties in transient transfection of human genes. Different cell lines were optimized to find the optimal ratio of DNA to transfection agent to express our protein of interest (ABCG5 and ABCG8). In addition to difficulties with transfection, optimization was needed to find an antibody that detected the human ABCG5/8 protein via Western Blotting.

Experimental Design: Each cell line was seeded on day zero, at varying sub-confluent densities in a 6 or 12-well dish. On day one, cells were transiently transfected using the ThermoFisher Scientific Lipofectamine 3000 kit according to their protocol. Transfections were performed initially at various ratios of DNA to Lipofectamine and then performed at a standard 1.5 µg DNA:2 µl Lipofectamine, 2 µg DNA: 2 µl Lipofectamine, and 3 µg DNA: 2 µl Lipofectamine. The Lipofectamine complexes were combined according to the manufacturer's protocol and incubated for 30 minutes at room temperature. Prior to adding the complexes to the cells, 200-300 µl of serum-free media was added to the cells. The complexes were added dropwise to the cells and incubated at 37°C for 1-3 hours before adding 1 ml of complete media. On day two, GFP lysates were prepared and analyzed as previously described.

After standardizing the concentration of DNA and Lipofectamine that would be utilized in subsequent experiments, each cell line was transfected at 2 µg DNA: 2 µl Lipofectamine on day one in the following conditions: GFP, GFP+G5, GFP+G8, G5+G8. On day two, the media was replaced and 1% Triton Lysates were made on day three.

Lysates were quantified by a BCA assay and Immunoblotted for protein detection of human ABCG8.

2.4 Experiment III- Mutant Maturation Assay

Purpose: Clinically confirmed ABCG8 mutations have different molecular mechanisms that cause a lack of function of ABCG5/8 to efflux sterols. In the mutant maturation assay, we are referring to the maturation of the protein from the synthesis in the ER to beyond the Golgi. This experiment was performed to see to what extent ABCG8 mutants matured beyond the ER (Fig. 2.4-1).

Figure 2.4-1 Graphical Representation of *in vitro* maturation assay.
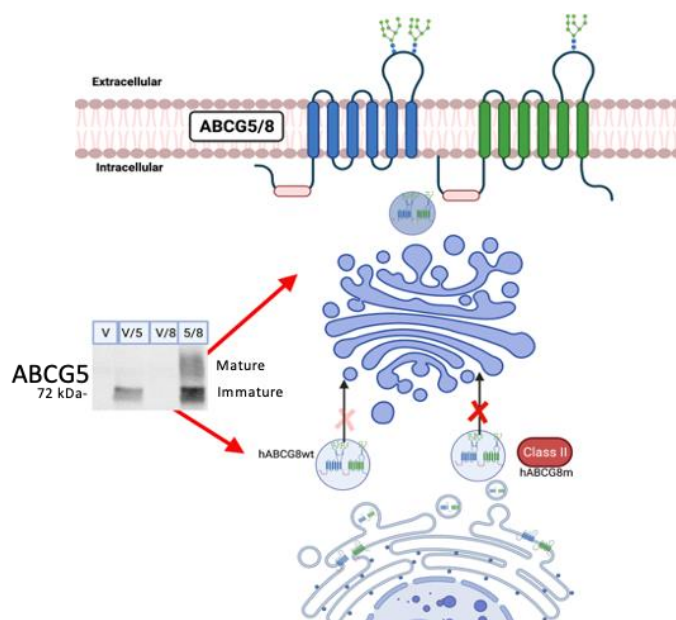
Figure 2.4-1. Graphical representation of in vitro assay to monitor ABCG8 maturation beyond the ER. Observing the change in electrophoretic mobility of ABCG8 or ABCG5 can be used as a marker for maturation, indicative of maturation competent or incompetent mutations (Class II).

Experimental Design: After mutants were generated and sequence verified, all mutants were prepped with the Qiagen Midi Prep Plus kit. Two independent cell culture experiments were conducted. In all experiments, HuH-7 cells were seeded at a sub-confluent density in a 6 or 12-well dish on day zero. In the first experiment, cells were transfected on day one with V, V+myc tagged-G5, V+G8, myc tagged-G5+G8, and native myc tagged-G5+mutant G8. Using a C-terminal myc tagged ABCG5 construct was to be able to monitor both G5 and G8 maturation, as during experimentation, we did not have a validated human ABCG5 antibody. In the second experiment, cells were transfected on day one with V, V+G8, myc tagged-G5+G8, and V+mutant G8 alongside a GFP loading control to monitor ABCG8 mutant stability in the absence of ABCG5. For all experiments, culture media was replaced the day following transfections, and 48 hours post-transfection,

Triton (1%) lysates were prepared. Lysates were analyzed through a BCA assay and analyzed as previously described.

Subsequent experiments include SalI digest (as previously described) and RNA extraction. The RNA extraction *in vitro* assay resembled the V+mutant hG8 stability assay, the only difference being that rather than lysing the cells with 1% triton, they were lysed with TRIzol (Life Technologies) and proceeded to be processed using the RNeasy kit from Qiagen. The RNA was transcribed into cDNA using the iScript Reverse Transcriptase kit. The cDNA was then amplified with forward and reverse primers utilized in the site-directed mutagenesis PCR reactions and ran on a 2% agarose gel containing .01% SYBRsafe.

2.5 Experiment IV- Native ABCG5/G8 Complex Compound Screening

Purpose: Based on previous experiments done in ABCC7 and ABCB4 transporters, Roscovitine along with its 11 analogs were tested to see if there was potential in increasing the maturation of the native ABCG5/8 complex.

Experimental Design: HuH-7 cells were seeded in two 12-well dishes at a sub-confluent density on day zero. On day one, cells were transfected with control V, V/G5, V/G8, G5/G8, and the remaining wells with G5/G8. On day two, cells were supplemented with low serum media (DMEM + .2% BSA) and either 100 uM of Roscovitine and analogs or .1% DMSO vehicle (Vauthier, 2019). On day three, 1% triton lysates were prepared and analyzed with a BCA assay. Lysates were Immunoblotted as previously described for ABCG8 and Calnexin.

2.6 Experiment V- Roscovitine Toxicity

Purpose: Based on previously published data on Roscovitine and its known toxicity, we wanted to observe further both the toxicity and impact on protein concentration when HuH-7 cells were treated with Roscovitine in a dose-dependent manner.

Experimental Design: On day zero, Huh-7 cells were seeded at a sub-confluent density in 6-well dishes. The cells received treatment media on day two. Treatment media composed of 0.2% BSA with added 1% Pen-Strep and 1% GlutaMAX. The five treatment conditions were: .1% DMSO, 100 uM Roscovitine, 20 uM Roscovitine, 5 uM Roscovitine, and 1 uM Roscovitine. On day 3, media was collected and centrifuged to remove cellular debris and triton lysates were prepared. An LDH Assay was performed on the media to measure toxicity and a BCA Assay was performed on the lysates to measure protein concentration.

2.7 Experiment VI- Corrector Testing of Class II Mutants

Purpose: After establishing a classification system for clinically found Sitosterolemia-associated cytosolic mutants in ABCG8, FDA-approved correctors (Luma-, Teza-, Elexacaftor) used in the treatment of Cystic Fibrosis were tested *in vitro* to observe if heterodimerization and trafficking beyond the ER could be restored in Class II mutants.

Experimental Design: Huh-7 cells were seeded in a 6-well dishes at sub-confluent density on day zero. On day one cells were transfected with control GFP, GFP/G5-GFP/G8- G5/G8 and the remaining wells with wildtype G5/mutant G8. On day two, cells were supplemented with low serum media (DMEM + .2% BSA) and six combinations of corrector treatments (Vehicle, Luma-, Teza-, Elexa-, Luma + Elexa, and Teza + Elexa) in previously used concentrations[68]. On day three, 1% triton lysates were prepared and analyzed for maturation.

2.8 Experiment VII- Immunofluorescence of Maturation Competent Mutants

Purpose: Mutants that are maturation competent or demonstrate a decrease in maturation were analyzed via immunofluorescent microscopy to observe if they are capable of trafficking to the cell surface in the presence of cycloheximide, a known protein synthesis inhibitor.

Experimental Design: Cells were seeded on coverslips, co-transfected with ABCG5-myc and either mutant and wildtype ABCG8. Cells were fixed and treated cells with the KWE5 (mouse anti-human ABCG8) and then a conjugated secondary fluorophore (goat anti-mouse 488 or goat anti-rabbit 568). Coverslips were mounted with a mounting medium that contained DAPI to label the nuclei and imaged under blue, red, and green fluorescence.

CHAPTER 3. RESULTS

We investigated cytosolic, missense mutations in *ABCG8* to determine if ABCG5/G8 dimerization and trafficking beyond the ER were compromised. After understanding the molecular defects of the mutants, we observed the effects of proteostasis regulators on the native ABCG5/G8 complex to observe whether or not the transporter dimerization could be enhanced. Further, we observed the effects of FDA-approved correctors (Luma-, Teza-, and Elexacaftor) in class II mutants of ABCG8. The results for each of the following are listed below.

3.1 Experiment I- Generation of Sitosterolemia-Associated ABCG8 Cytosolic Mutants

We generated 9 cytosolic, Sitosterolemia-associated mutants in ABCG8 via site-directed mutagenesis (Fig. 3.1-1). The mutations we generated were clinically found in patients with a biochemical diagnosis of Sitosterolemia. The purpose of generating these missense mutations was to observe the effects of the mutations *in vitro* in human hepatocytes, as seen in Experiment III. Using site-directed mutagenesis allowed us to make a single base pair change to introduce our desired mutation without altering the remainder of the protein.

The native ABCG8 construct was used as a negative control throughout the site-directed mutagenesis to ensure that the only bacterial growth post-transformation was PCR product and not the original plasmid (DpnI digest). The native ABCG8 construct was also used as a positive control in the SalI restriction enzyme digest to confirm that our mutant constructs did not have significant structural changes in the DNA. This process was described in the methods section.

36

Figure 3.1-1 ABCG8 Mutation Diagram
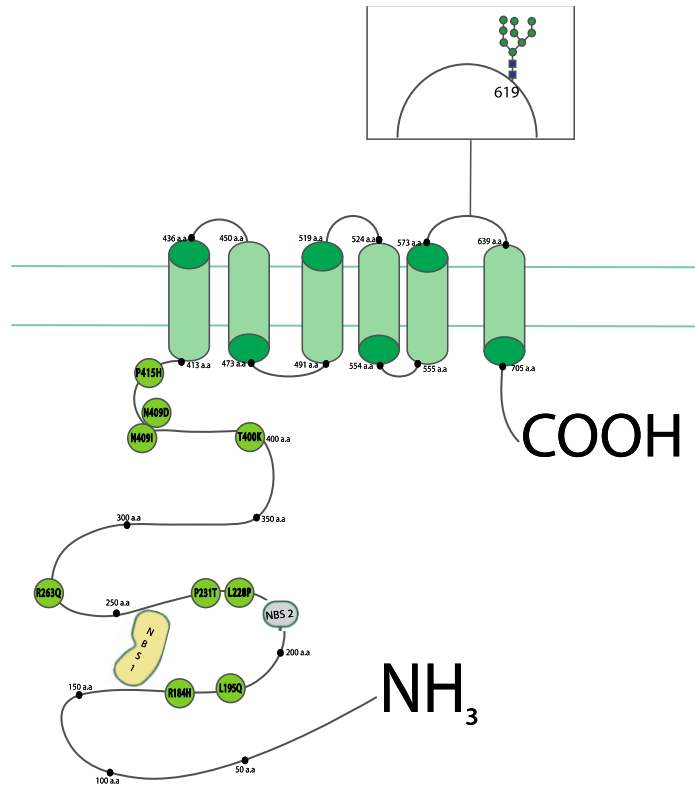
Fig. 3.1-1 Diagram of the ABCG8 transporter and Sitosterolemia mutations placed in the corresponding location on the transporter. Amino acid 619 represents the glycosylation site for ABCG8.

Additionally, Bioinformatic analysis of these nine mutations are shown in Figure 3.1-2 and 3.1-3. The protein analysis shown is both comparisons of ABCG8 across species and between the ABCG Family of transporters.

Figure 3.1-2. ABCG8 Sequence conservation among species.

```
180-240 A.A.              R184H          L195Q                              L228P P231T
>H. sapiens             SQAQRDKRVEDVIAELRLRQCADTRVGNMYVRGLSGGERRRVSIGVQLLWNPGILILDEP
>M. mulatta             SQAQRDKRVEDVIAELRLRQCADTRVGNTYVRGVSGGERRRVSIGVQLLWNPGILILDEP
>C. lupus familiaris    SQAQRDQRVDDVIAELRLRQCANTRVGNAYVRGVSGGERRRVSIGVQLLWNPGILILDEP
>M. musculus            SQAQRDKRVEDVIAELRLRQCANTRVGNTYVRGVSGGERRRVSIGVQLLWNPGILILDEP
>D. rerio               SQKQRDQRVDDVIAELRLRQCAHTRVGNEYVRGVSGGERRRVSIAVQLLWNPGILILDEP


258-269 A.A.              R263Q
>H. sapiens             LAKGNRLVLIS
>M. mulatta             LAKGNRLVLIS
>C. lupus familiaris    LAKGNRLVLVS
>M. musculus            LAKGNRLVLIS
>D. rerio               LARGNRLVLLS


390-420 A.A.              T400K     N409D/I P415H
>H. sapiens             AVQQFTTLIRRQISNDFRDLPTLLIH
>M. mulatta             AVQQFTTLIRRQISNDFRDLPTLLIH
>C. lupus familiaris    PVQQFTMLIRRQIFNDFRDLPTLLIR
>M. musculus            MIEQFSTLIRRQISNDFRDLPTLLIH
>D. rerio               KVHQFTTLIRRQVFNDYRDLVTLVVH
```

Fig. 3.1-2. Sequence alignment using FASTA files from NCBI (Source) and Snapgene 4.3.11. Species aligned in order top to bottom are human, Rhesus monkey, Dog, Mouse, Zebrafish. Mutants in the analysis are in bold, yellow highlighted residues are conserved while green are not conserved.

Figure 3.1-3. ABCG8 Sequence conservation among ABCG family members.

```
180-240 A.A.   R184H      L195Q                              L228P P231T
>hABCG1      KDEGRREMVKEILTALGLLSCANTRTGS-----LSGGQRKRLAIALELVNNPPVMFFDEP
>hABCG2      TNHEKNERINRVIQELGLDKVADSKVGTQFIRGVSGGERKRTSIGMELITDPSILFLDEP
>hABCG4      KQEVKKELVTEILTALGLMSCSHTRTAL-----LSGGQRKRLAIALELVNNPPVMFFDEP
>hABCG5      NPGSFQKKVEAVMAELSLSHVADRLIGNYSLGGISTGERRRVSIAAQLLQDPKVMLFDEP
>hABCG8      SQAQRDKRVEDVIAELRLRQCADTRVGNMYVRGLSGGERRRVSIGVQLLWNPGILILDEP
258-269 A.A.   R263Q
>hABCG1      LAQGGRSIICTI
>hABCG2      MSKQGRTIIFSI
>hABCG4      LAQGGRTIICTI
>hABCG5      LARRNRIVVLTI
>hABCG8      LAKGNRLVLISL


390-420 A.A.   T400K      N409D/I P415H
>hABCG1      CLTQFCILFKRTFLSIMRDSVLTHLR
>hABCG2      FCHQLRWVSKRSFKNLLGNPQASIAQ
>hABCG4      TLTQFCILFKRTFLSILRDTVLTHLR
>hABCG5      VFSKLGVLLRRVTRNLVRNKLAVITR
>hABCG8      AVQQFTTLIRRQISNDFRDLPTLLIH
```

Fig. 3.3-1. Sequence alignment using FASTA files from NCBI (Source) and Snapgene 4.3.11. ABCG8 Family members include 1, 2, 4, 5, and 8. Mutants in the analysis are in bold, yellow highlighted residues are conserved while green are not conserved.

3.2 Experiment II- Optimization of Transient Transfection of Human Cell Lines

For transient transfection *in vitro,* there are different transfection reagents commercially available, both liposome and non-liposome. In a series of transfection optimization experiments, we observed differences in transfection efficiency between three different reagents; Lipofectamine 3000, FuGene6, and Endofectin Max in our HuH-7 system. HuH-7 cells are a human hepatocarcinoma cell line that have been reported to have optimal transfection efficiency as well as potential applications with polarization. Ratios were determined by previously published studies done in HuH-7 cells for FuGene6 and Endofectin[70]. GFP signal was quantified by fluorescence reading of 485 nm excitation and 515 nm emission and normalized to the A_{280} (arb. units). The densitometric analysis was done in Adobe Photoshop and quantified by a ratio of Mature to Immature signal and expressed as GFP signal vs. Maturation Index for the ABCG5 blot.

Figure 3.2-1 Comparison of different transfection reagents in the HuH-7 cell line.
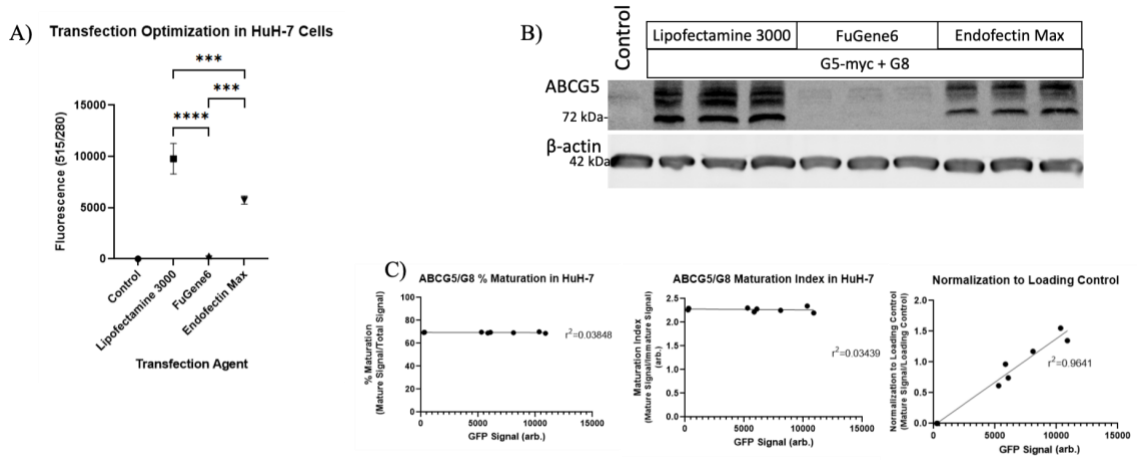
Fig. 3.2-1. A. Huh-7 cells transfected with ~2 ug of DNA (1 ug hG5-myc, 1 ug hG8, 100 ng GFP) and 4 ul of transfection reagent (Lipofectamine 3000, FuGene6, and Endofectin Max) in triplicates. Samples were analyzed by GFP fluorescent detection expressed as 515/A280 and a same day control lysate was background subtracted. Data was analyzed by a One-way ANOVA and significant differences were determined by Tukey Post-Hoc, * p<.05, ** p<.01, *** p<.001, ****p<.0001. B. Western blot of lysates prepped to confirm transfection efficiency was synonymous with signal intensity, with C) regression analysis on the % Maturation, Maturation Index, and Normalization to Loading Control.

From initial transfection optimization experiments, it was determined that at the concentrations of DNA and volume of transfection reagents we tested, the HepG2 cells had the lowest transfection efficiency while Huh-7 and HEK293 cells had comparable transfection efficiencies. Because our desired experimental cell line are hepatocytes and due to HEK293's poor adherence and inability to tolerate compounds, these findings led us to continue the remainder of our *in vitro* experiments in the Huh-7 system, with transfection optimization shown below (Fig. 3.2-2). No statistical differences were detected across various volumes of Lipofectamine or plasmid DNA. Previous optimizations in other cell lines determined 2 ug plasmid DNA to 2 ul Lipofectamine was the optimal ratio and therefore we selected a 1:1 ratio to stay consistent with conditions used in other cell lines in the lab.

Figure 3.2-2 Transfection Optimization in HuH-7 cells.
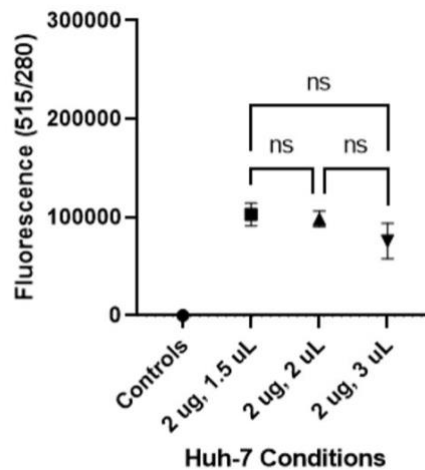
Fig. 3.2-2 Transfection efficiency in the Huh-7 Cells transfected with the same concentration of DNA (2 ug of GFP) and varying volumes of Lipofectamine. Samples were ran in triplicate on a 12 well dish. Data was analyzed with a One-way ANOVA and a Tukey's post-hoc test.

3.3 Experiment III- Mutant Maturation Assay

The findings from the mutant trafficking assay determined that

approximately 44% of ABCG8 were maturation incompetent. We determined this by

monitoring the upper molecular weight form of ABCG8, which indicates that the protein

has been glycosylated and matured beyond the ER. Transmembrane proteins become

glycosylated during trafficking from the ER to the Golgi and are further modified as the

protein transits the Golgi. The bulky moiety causes a shift in molecular weight, an

indicator of protein maturation. We monitored ABCG8 mutant maturation in 3 ways:

tracking ABCG8 maturation, tracking ABCG5 maturation, and the stability of the

ABCG8 mutants in the absence of their partner. The densitometric analysis was

completed by using the measurement feature in Adobe Photoshop and using the

integrated density as a measurement for signal intensity. In this particular assay, we

expressed the signals as a percent (mature signal/total signal) and as an index (immature

41

signal/mature signal) using the ABCG5 blots. Due to the appearance of a high upper molecular weight band (*), the ABCG8 blot was not included in the densiometric analysis.

Figure 3.3-1. Protein maturation bioassay demonstrating ABCG8 cytosolic mutants co-transfected with ABCG5-myc.

Figure 3.3-1. Huh-7 cells transfected with Controls and native hG5-myc/mutant hG8. A) Western blot depicts in vitro trafficking assay, with B) Densiometric analysis for % maturation (Mature Signal/Total Signal) and Maturation index (Mature Signal/Immature Signal). The % maturation was internally normalized to GFP. Data (n=3) was analyzed by a One-way ANOVA with a Dunnett's Post-hoc test. (*) $p<.05$, (**) $p< .01$, $p<.001$ (***), $p<.0001$ (****).   C) Normalization to loading control of the one experiment shown (n=1).

From this maturation assay, it was apparent that in the mutants with a statistically significant reduction in maturation in the ABCG5 blots, a signal was not detected in the ABCG8 blot. Additionally, we investigated the stability of mutants in ABCG8 by expressing the mutants in HuH-7 cells in the absence of ABCG5. The blots (shown below) demonstrated the same pattern of apparent Class II mutants lacking the ABCG8 immature signal.

Figure 3.3-2. Protein stability Western blots of mutants in ABCG8.
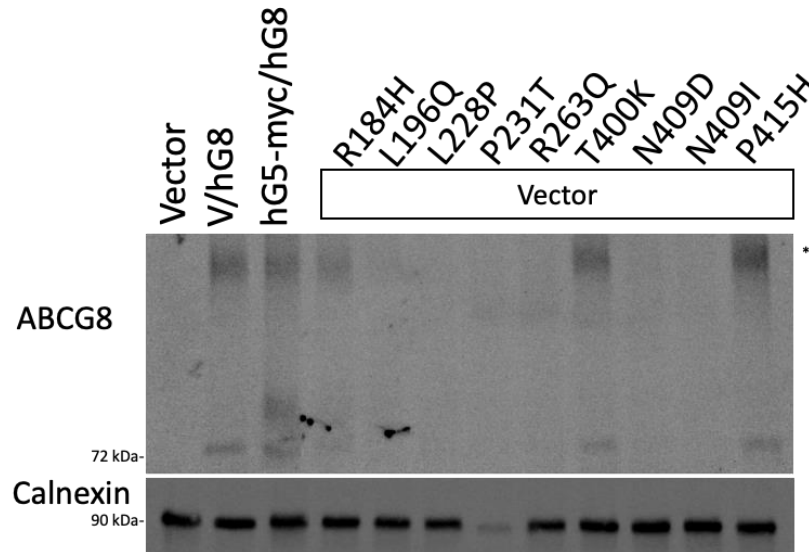
Fig. 3.3-2 Huh-7 cells transfected with vector and mutant hG8 in the absence of hG5. Western blot depicts in vitro stability of the monomer compared to native hG8 and native ABCG5/G8.

We then asked two questions; did our DNA plasmid preps contain DNA at the concentration the spectrophotometer was giving out? Furthermore, was the DNA being transcribed into RNA? We knew the protein was not expressed due to the lack of signal in the ABCG8 blots. The first experiment to test these was a restriction enzyme digest using SalI to confirm we had DNA and to verify there were no significant structural changes compared to wildtype ABCG8.

Figure 3.3-3**.** Restriction enzyme digest on Class II mutants.
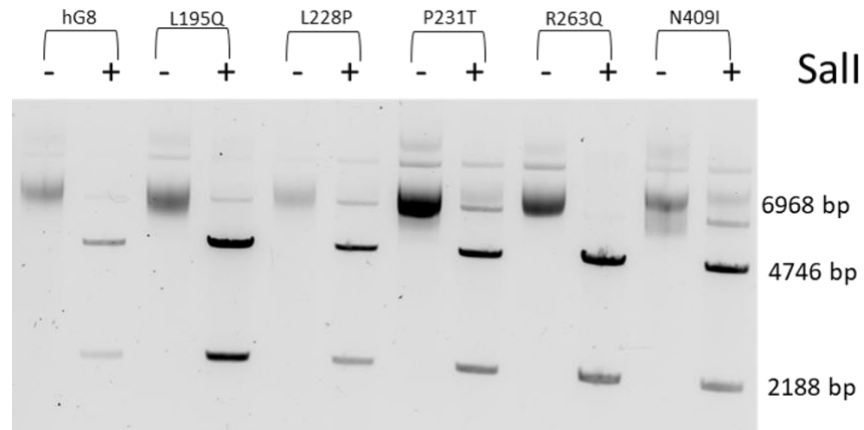
Figure 3.3-3. Restriction enzyme digest of wildtype ABCG8 and mutant ABCG8. Samples were digested using SalI on a thermocycler block and analyzed on a 1% agarose gel and fluorescently imaged via SYBRsafe.

After the restriction enzyme digest and gel electrophoresis, we concluded

that while signal intensity did vary mutant to mutant, there was in fact, DNA in our

plasmid prep. We seeded HuH-7 cells at a sub-confluent density on day zero, day one

transfected cells with vector and either hG8 or Class II mutant hG8, and treated cells with

Trizol on day two. We extracted RNA using the Qiagen RNA extraction kit. After RNA

extraction, cDNA was generated using reverse transcriptase and the amplicons were

analyzed on a 2% agarose gel (Fig. 3.3-4).

Figure 3.3-4. Gel electrophoresis of cDNA from HuH-7 lysates
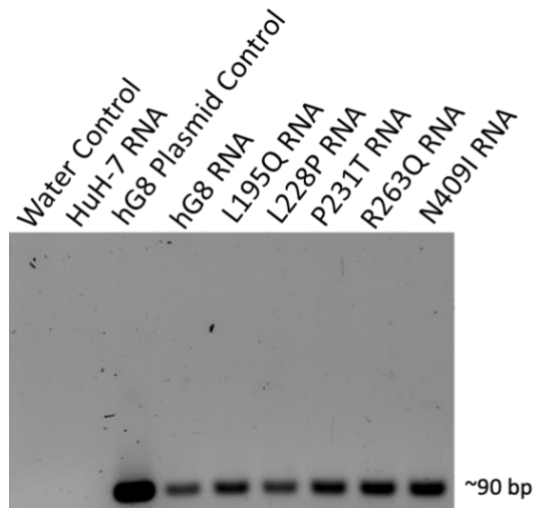
Figure 3.3-4. cDNA of wildtype ABCG8 and mutant ABCG8 amplified and analyzed on a 2% agarose gel and fluorescently imaged via SYBRsafe. Samples were lysed from HuH-7 cells, extracted RNA, transcribed cDNA, and amplified using SYBRgreen.

3.4 Experiment IV-Corrector Testing of Class II Mutants

In testing the CFTR correctors on the Class II maturation deficient mutants, we determined in the conditions we tested, that the CFTR modulators were unable to "correct" maturation deficient mutants in the cytosolic domain of ABCG8. Figure 15 is an example of the full screen for each mutant (R263Q) and the two dual therapies (Lumacaftor and Elexacaftor or Tezacaftor and Elexacaftor) on all maturation incompetent or maturation comprised mutants.

Figure 3.4-1 Protein maturation bioassay with treatment with published concentrations of CFTR correctors[68].
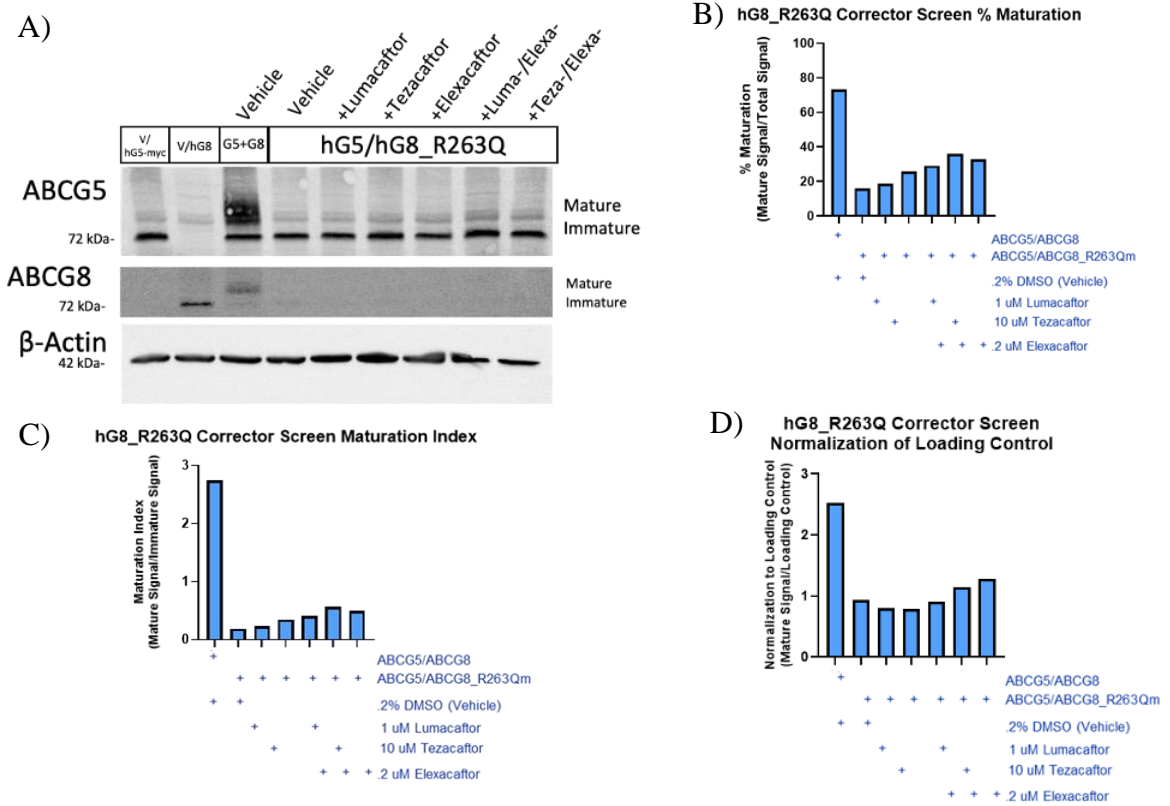
Fig. 3.4-1. Huh-7 cells transfected with native hG5-myc/mutant hG8 with treatment of CFTR correctors at published concentrations. A) Western blot depicts in vitro trafficking assay in HuH-7 cells, with B) Densiometric analysis for % maturation (Mature Signal/Total Signal), C) Maturation index (Immature/Mature Signal), and D) Normalization to loading control (Mature Siganl/B-actin).

3.5 Experiment V- Testing Regulators of Proteostasis on Native ABCG58

Roscovitine and the 11 analogs synthesized were tested on both HuH-7 (Fig. 16) and HepG2 cells (Fig. 17). The densitometric analysis demonstrates in both cell lines these 12 treatments at 100 uM, specifically on the MRT2-237-245 compounds, an increase in maturation compared to the native complex. Throughout testing these compounds at a 100 uM concentration, patterns of low protein yield in cell lysates as well as acidification of the media (yellow) media, suggesting cell lysis. We proceeded to run

an LDH activity assay to determine a concentration where Roscovitine, the most

observed toxic compound, had a reduced level of LDH activity (see results in Experiment

VI).

The results of experiment VI led to reducing the regulator of proteostasis screen

from 100 uM to 20 uM in an attempt to retain the cell morphology during culturing. The

results of the 20 uM experiments are ongoing.

Figure 3.5-1. Roscovitine Screening on native ABCG5/G8 complex in HuH-7 cells at 100
uM.
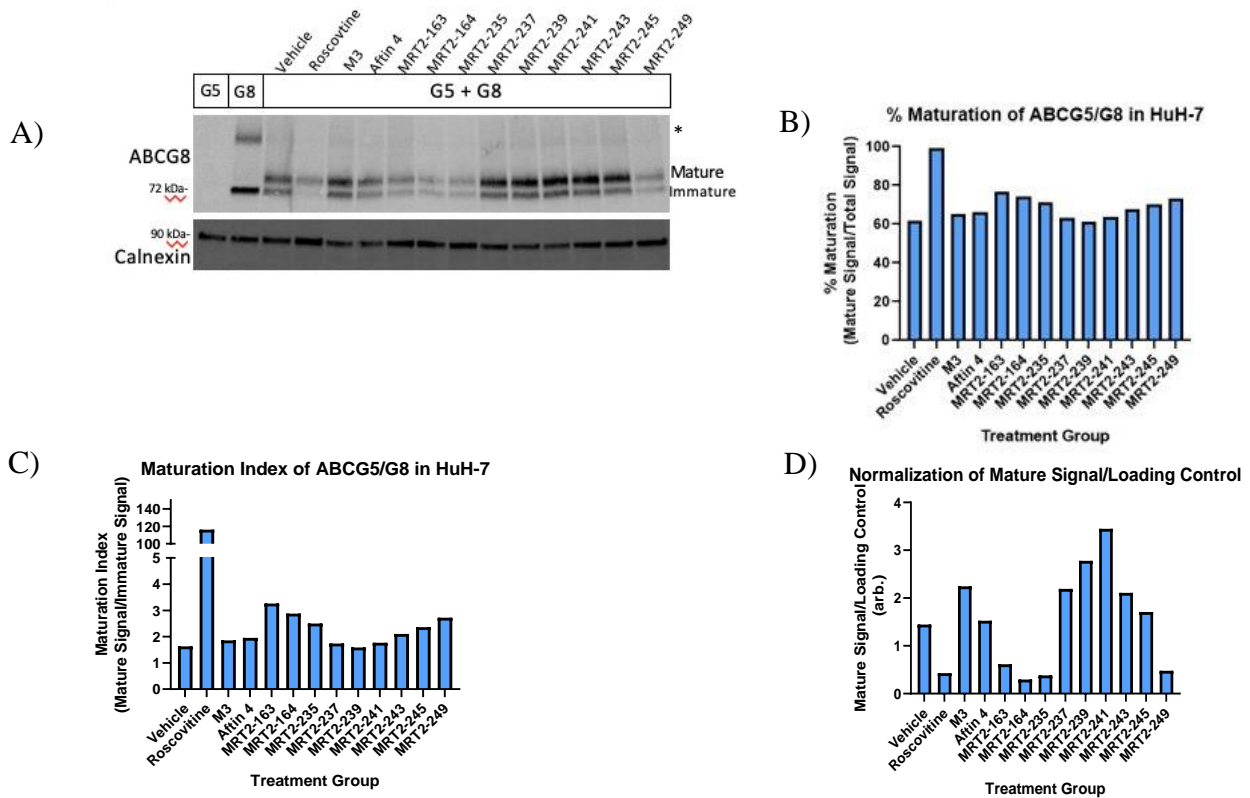
Fig. 3-5.1. HuH-7 cells transfected with native hG5-myc/hG8 with treatment of Roscovitine and 11 analogs at 100 uM. A) Western
blot depicts in vitro trafficking assay in HuH-7 cells, with B) Densiometric analysis for % maturation (Mature Signal/Total Signal), C)
Maturation Index (Mature Signal/Immature Signal), and D) Normalization to the loading control (Mature Signal/Calnexin). The
following blot does not have an internal GFP standardization or statistical analysis (n=1).

Figure 3.5-2. Roscovitine Screening on native ABCG5/G8 complex in HepG2 cells at 100 uM.
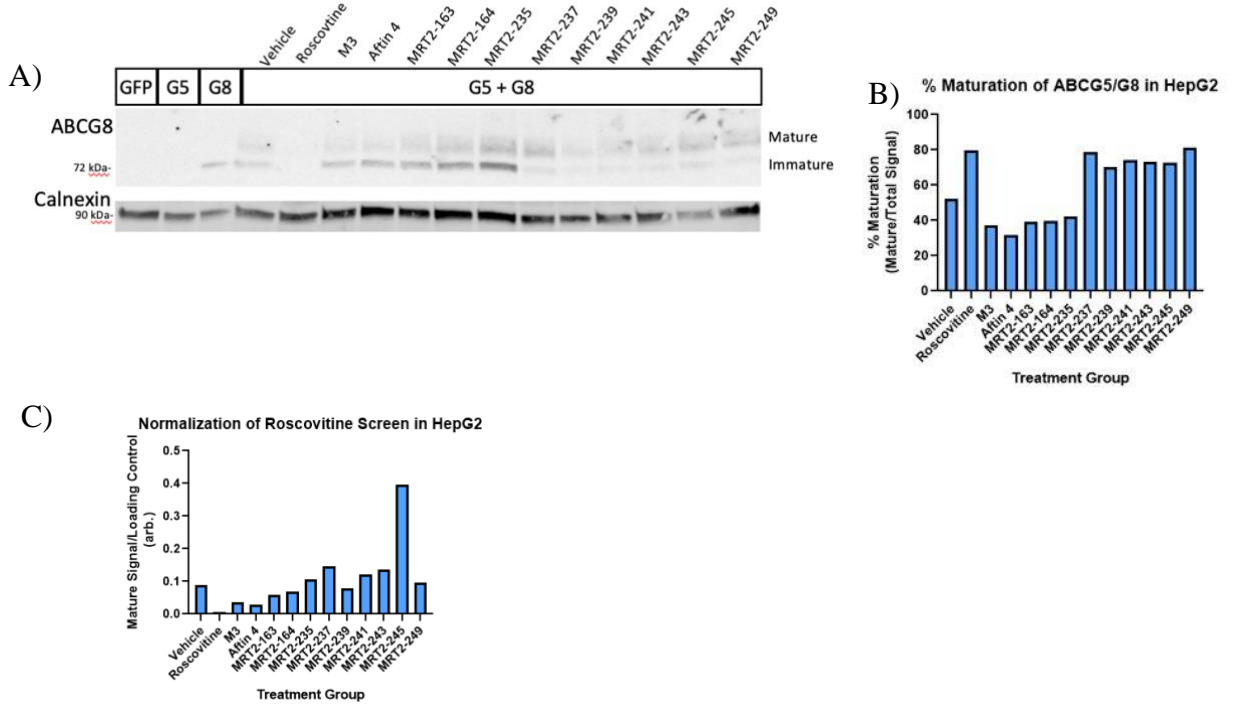
Fig. 3.5-2 A. Western blot depicts in vitro trafficking assay in HepG2 cells when treated with 100 uM Roscovitine and analogs. B. Densiometric analysis for % maturation (Mature Signal/Total Signal) and C. normalization to the loading control (Mature Signal/Calnexin). n=1.

3.6 Experiment IV- Roscovitine Dose-Response

From previously published experiments and based on difficulties retaining a high protein concentration in lysates from Roscovitine, we wanted to observe the toxicity of Roscovitine both in LDH activity as well as its impact on protein concentrations. Using a LDH activity assay, we measured both LDH activity and toxicity of Roscovitine at four doses. (Fig. 18). Based on these experiments, we elected to proceed with a concentration of 20 uM in the HuH-7 system due to the reduced toxicity and LDH activity as well as increased protein concentration.

Figure 3.6-1 Dose-Response data on Roscovitine in HuH-7 cells.
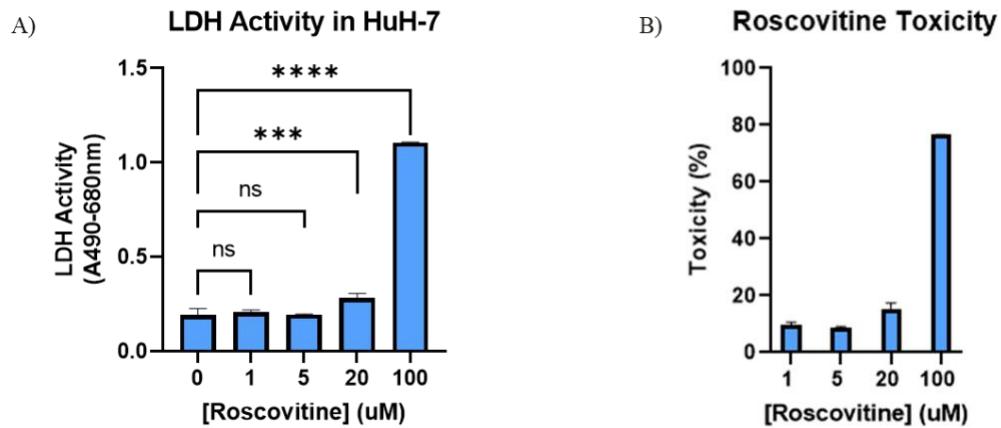
Fig. 3.6-1 A. HuH-7 cells were treated in a dose-dependent manner with Roscovitine, a compound that has shown toxicity in multiple cell lines in our hands as well as published by other research groups. The data was expressed as LDH Activity (A_{480}-A_{690}) vs. concentration of compound. B. Toxicity of Roscovitine calculated with max LDH activity and negative control of vehicle treated cells. LDH Activity was analyzed by a One Way ANOVA and with a Dunnett's Post-hoc test (n=3).

3.7 Experiment VI- Immunofluorescence Trafficking Assay

As described in the methods section, HuH-7 cells were processed for immunofluorescence microscopy. Initially, we tested the native ABCG5/G8 complex in a cycloheximide time course experiment. We treated cells with 50 ug/ml cycloheximide for 1 hour, 2 hours, 4 hours, 8 hours, and overnight as well as a non-treated well (Fig. 3.7-1).

Figure 3.7-1. Immunofluorescence and images from the cycloheximide time course experiment.
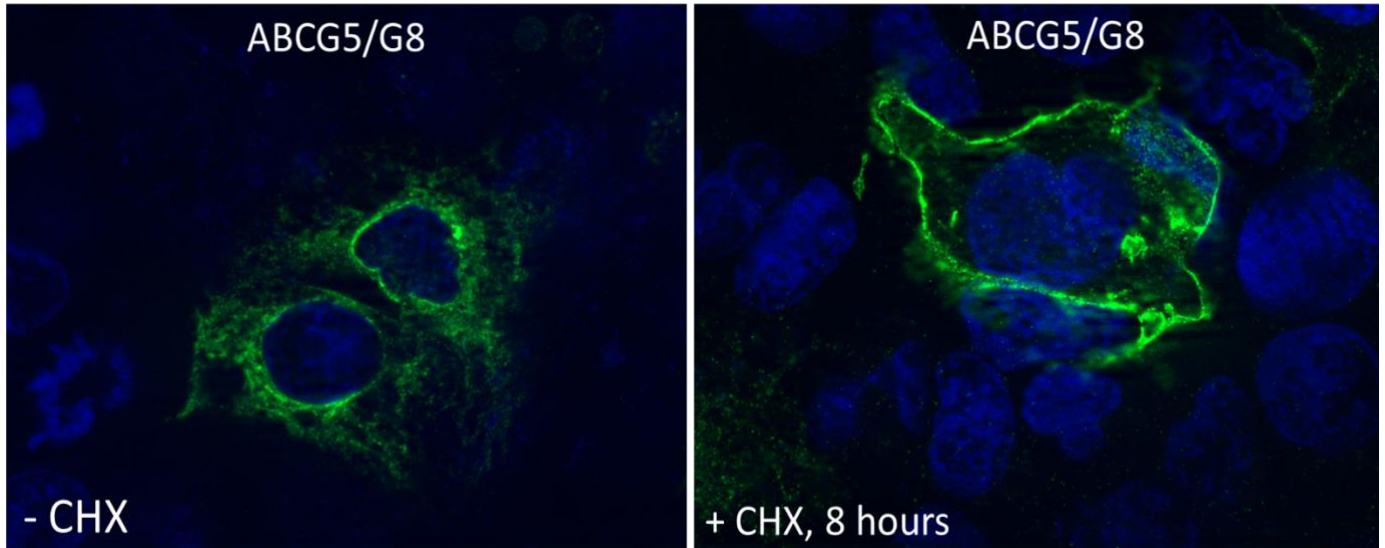
Fig. 3.7-1 HuH-7 cells were transfected with native G5G8. Cells were then treated at different time points with 50 ug/ml cycloheximide. The two images shown are representative images of our negative control, without cycloheximide treatment, and the time point we continued experimentation with, 8 hours. Cells were stained for ABCG8 (KWE5 lot-1), AlexaFluor-488. Images are slices taken at 100X with Zeiss Axiovert 200M using the Apotome camera for confocal microscopy.

Additionally, we did a time-course using 50 ug/ml and 100 ug/ml of cycloheximide to monitor ER depletion and analyzed with SDS-PAGE and Immunoblotting as previously described (Fig. 3.7-2).

Figure 3.7-2. Time-course with 50 and 100 ug/ml CHX.
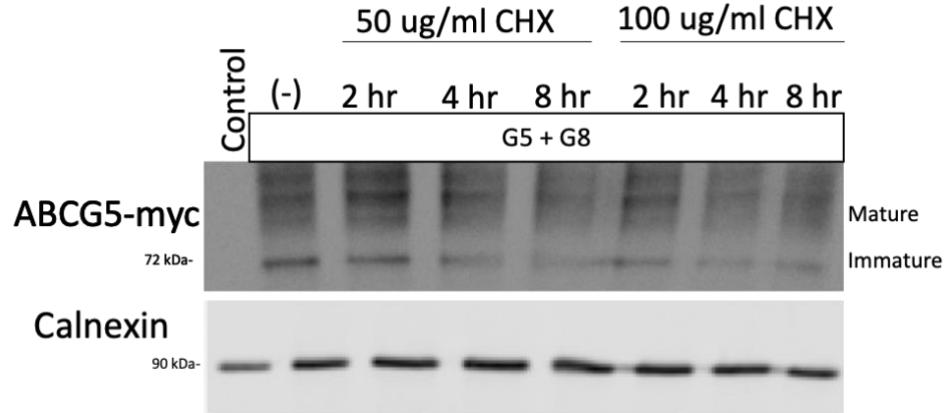
Fig. 3.7-2. HuH-7 cells were transfected with native G5G8. Cells were then treated at different time points with 50 ug/ml OR 100 ug/ml cycloheximide. Cell lysates were analyzed by SDS-PAGE and immunoblotted for ABCG5 with a c-myc antibody and calnexin loading control.

After these cycloheximide time-course experiments, we concluded that 50 ug/ml of cycloheximide at 8 hours was the optimal dose and time at the conditions that we tested. We then transfected HuH-7 cells with the maturation competent ABCG8 mutants to investigate whether they were capable of localizing to the plasma membrane or not.

Figure 3.7-3 Immunofluorescence images of ABCG8 mutants.
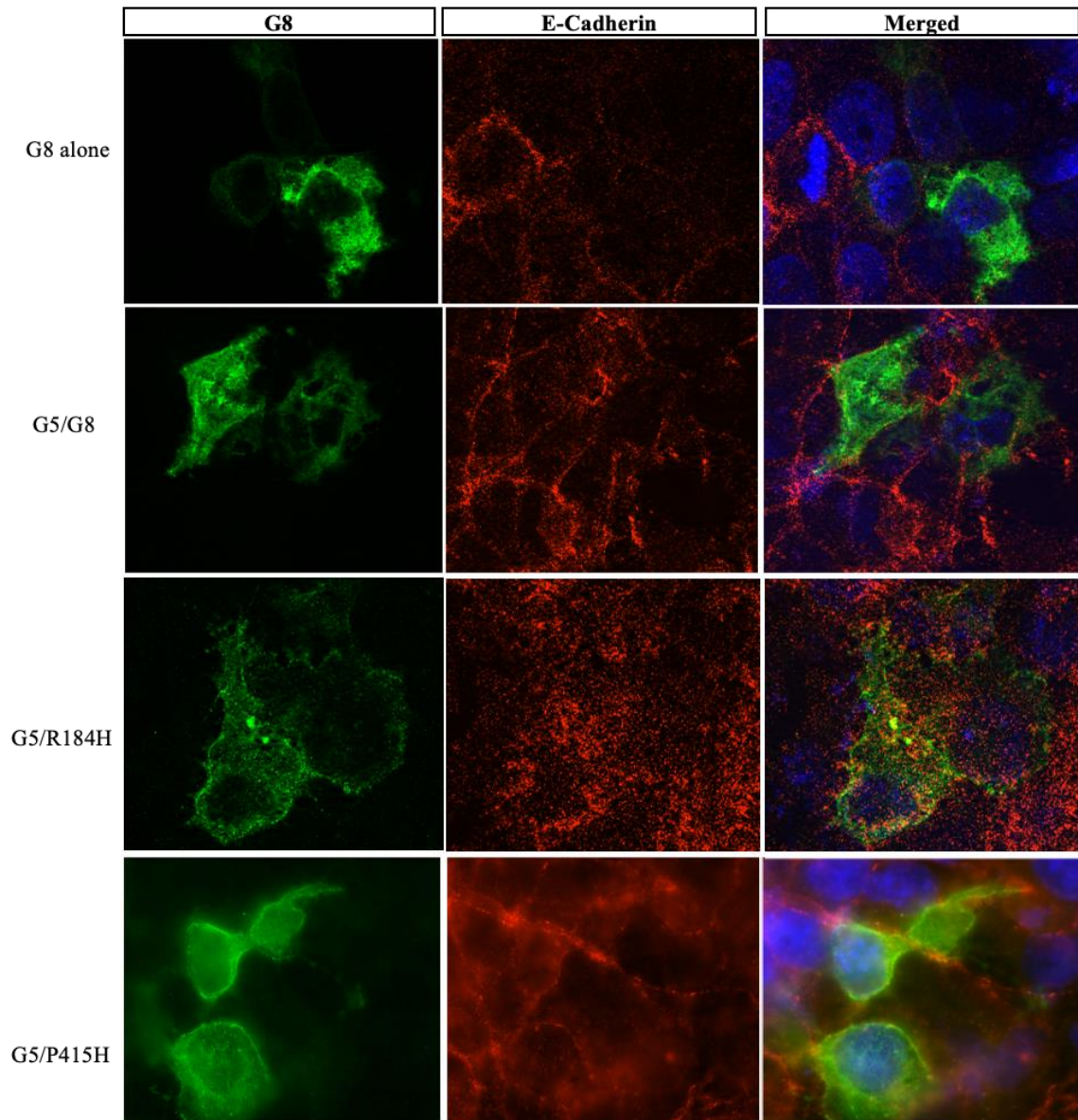
Fig. 3.7-3. HuH-7 cells were transfected with G8 control, native G5G8, or mutant G8 co-transfected with wildtype G5. Cells were then treated 50 ug/ml cycloheximide for 8 hours. Cells were stained for ABCG8 (KWE5 lot-1) and AlexaFluor-488, E-cadherin and AlexaFluor-568, and DAPI. Images are slices taken at 100X with Zeiss Axiovert 200M using the Apotome camera for confocal microscopy.

The results from the analysis of the Immunofluorescence microscopy was mutants R184H and T400K exhibited a trafficking pattern that resembled the wildtype complex while N409D, N409I, and P415H appeared to localize to some subcellular compartment

that was distinct from the wildtype. Representative images are shown in Figure 3.7-3 of

one mutant that had apparent trafficking or trafficking to another subcellular

compartment.

Our protein of interest is endogenously expressed at high levels in the liver (hepatocytes) and small intestine (enterocytes). Both of these cell types have known difficulties for *in vitro* assays, particularly that they are not easily transfected. Because of the nature of the project, we needed to find a cell line that could be efficiently transfected and had a translational relationship. Initially, we began our analysis in HepG2 cells. These are another human hepatocyte cell line, and while they can be polarized, their ability to transfect our gene of interest was sub-optimal. We then moved into a well-established cell line successful in transient transfections, HEK293 cells. While these cells were not our desired model system, they could express our proteins in high abundance and were easily detected via immunoblotting. However, because HEK293 cells are a loosely adherent cell type, they could not withstand compound testing when treated at 100 uM of the Roscovitine screening. This finally led us to our working system of HuH-7 cells. HuH-7 cells are a human hepatocarcinoma cell line that has been described as a viable substitute to primary hepatocytes. Their transfection efficiency exceeds HepG2, comparable to the HEK293 cells, and could tolerate compound testing. The cons to the HuH-7 system was that in our hands, did not appear to polarize.

ABCG5 and *ABCG8* are known to be the two genes to cause Sitosterolemia[30]. In these experiments, we have begun a characterization of clinically published Sitosterolemia-associated mutants in the cytosolic domain of ABCG8. Additionally, we investigated potential therapies that could not only treat Sitosterolemia patients but also

open a door for several other ABC transporter-caused diseases. Experiments in this thesis led to the classification of 9 cytosolic mutants in ABCG8. In our *in vitro* experiments, we were able to classify the mutants into three classes; Class II, Class V, or unclassified. *In vivo* or *in vitro* (polarized cells) experimentation would be required to classify any unclassified mutants further. After the mutants were classified, Class II mutants were further investigated for the effects after treatment with CFTR correctors to observe if these mutants could be stabilized and traffic beyond the ER and thus "corrected."

Regulators of proteostasis were tested on the native ABCG5/8 complex to observe if there could be enhancement to an already poor-folding protein complex. In our hands, the Roscovitine analogs demonstrated modest increases in maturation, but the interesting story is the increased mature signal compared to the native complex. While one could argue that this could be due to changes in transfection efficiency, our GFP signal was utilized as an internal measure for differences in transfection across the wells. Because the mechanism of action of these analogs are thought to be inhibition of the proteasome, specifically with the Class II mutants that appear to be rapidly degraded, we can hypothesize that these compounds could provide some benefit to both native ABCG5/G8 as well as Class II maturation deficient mutants of ABCG8.

During our western blotting antibody troubleshooting, which will be further discussed in the limitations, we were monitoring G8 maturation through the c-myc tag on ABCG5. We probed the blots for ABCG8 with a KWE5 subclone of IB10A5 and noticed an ABCG8-specific banding pattern. A consistent pattern of a high molecular weight band (>100 kDa) appeared in the G8 only lane and for the majority resolved in the co-transfected lane but at a reduced signal. This phenomenon became apparent to us when

using the HuH-7 cells, as previously in the HepG2 or HEK293 cells we were having either low transfection efficiency or lower protein concentrations loaded on our SDS-PAGE gels (respectively). Additionally, this higher molecular weight banding pattern skewed the densitometric analysis due to the appearance of unresolved protein. The ABCG5 blots did not exhibit this high molecular band as seen in the ABCG8 blots. This is particularly interesting to study further as it could reveal a regulation of ABCG8 independent of ABCG5.

Approximately 44% of the mutants tested are maturation incompetent (Class II); L195Q, L228P, P231T, and R263Q. In addition to these four mutants, two exhibited a reduced level of maturation compared to the parent, R184H and N409I. None of the mutants that did not mature beyond the ER could be rescued with the CFTR modulators at this time. Of the remaining cytosolic mutants, we could not determine if any could localize to the plasma membrane with the tools we utilized. However, three of the maturation competent mutants, N409D, N409I, and P415H, appeared to localize to a subcellular vesicular compartment. The identity of this compartment will require further studies.

Table 4.6. Updated Sitosterolemia Classification system for mutants[52].

CLASS	DESCRIPTION	ABCG8 MUTANTS
I	Nonsense, Frameshift, Deletion	58 known or predicted
II	Maturation	L195Q, L228P, P231T, R263Q
III	Activity	
IV	Stability	
V	Trafficking	N409D, N409I, P415H
Unclassified	Inconclusive Results	R184H, T400K

Table 4.6. Updated Sitosterolemia classification system for mutants analyzed in this thesis.

4.1 Limitations

In our experimentation, there were a few limitations to our research. The first major limitation was that there are no commercial antibodies that recognize human ABCG5 and virtually only one antibody that is available commercially to recognize human ABCG8. For this reason, most of the blots were done with co-transfected human ABCG8 with a C-terminus myc-tagged human ABCG5 construct and immunoblotted with a c-myc antibody. However, because the myc tag is on the C-terminus and the glycosylation sites sit on the third extracellular loop of G5, we have no reason to believe this tag had any influence on our maturation bioassay. Towards the end of the thesis project, the lab had successfully grown and cultured the 1B10A5 hybridoma, which was producing a suitable amount of antibody to conclude the remainder of the immunoblotting and immunofluorescence experiments.

Another limitation we had for these experiments was in the generation of the cytosolic mutants in ABCG8. Because these are clinically published mutations, we had no control over the surrounding DNA when designing our oligos for the PCR reaction. The only components that were in our control were the annealing temperature, the size of the oligo, and the placement of the oligos with respect to where the point mutation occurred. For this reason, some mutants were more difficult than others based on the flanking DNA sequence.

4.2 Future Directions

In the HuH-7 system, we hypothesize that the likely source of this high molecular banding pattern observed in ABCG8 could result from a post-transcriptional modification, such as Ubiquitination, SUMOylation, or even rapid lysosomal degradation. Ongoing experiments to explore this upper molecular band include cell treatment with Chloroquine, a known lysosomal inhibitor. Ubiquitination and SUMOylation will be explored by Immunoprecipitation experiments to see if either Ub or SUMO will be pulled down alongside ABCG8.

Currently, the two Sitosterolemia treatment approaches still have experimentation to be completed to determine whether or not they could restore ABCG5 and ABCG8 function. At this time we do not have a positive control for CFTR and the CFTR delF508 mutant system or the ABCB4 mutants in hand to use as a positive control for Roscovitine and the analogs which is a current ongoing experiment. While Roscovitine was first tested in the F508del mutant, the analogs were tested in mutants of ABCB4. Having that as a positive control to continue to test the Class II ABCG8 mutants with these

compounds would be necessary as the previously published data was in HepG2 and HEK293 cells. Testing a handful of the analogs that show promise in enhancing the native ABCG5/8 complex on the Class II mutants would be the next direction in finding a treatment option for Sitosterolemia.

Additionally, the proteostatic regulator impact on the native ABCG5/G8 complex is intriguing, independent of Sitosterolemia. We can hypothesize that the enhancement seen in the screen of Roscovitine and analogs would lead to an increase in protein in the tissue in vivo. Additional experiments that would follow these results would include dose-response and time course experiments *in vitro*, *in vivo* administration of the compounds, and pharmacokinetic/pharmacodynamics experiments.

The future directions for these mutants are to further classify them beyond maturation and trafficking to the cell surface. First, we want to take a more quantitative approach to distinguish whether mutants can traffic to the plasma membrane *in vitro.* One planned assay is to biotinylate G8 to calculate the percentage of G8 on the cell surface. The following steps would be for *in vivo* experimentation to observe the activity of these mutants and *in vitro* polarization experiments would be required to study if these mutants' traffic to the apical membrane.

REFERENCES

1. Hubacek, J. A., Berge, K. E., Cohen, J. C., & Hobbs, H. H. (2001). Mutations in ATP-cassette binding proteins G5 (ABCG5) and G8 (ABCG8) causing sitosterolemia. *Human mutation*, *18*(4), 359–360. https://doi.org/10.1002/humu.1206
2. Zein, A. A., Kaur, R., Hussein, T., Graf, G. A., & Lee, J. Y. (2019). ABCG5/G8: a structural view to pathophysiology of the hepatobiliary cholesterol secretion. *Biochemical Society transactions*, *47*(5), 1259–1268. https://doi.org/10.1042/BST20190130
3. Ikeda, S., Mochizuki, A., Sarker A.H., Seki, S. Identification of Functional Elements in the Bidirectional Promoter of the Mouse Nthl1 and Tsc2 Genes,Biochemical and Biophysical Research Communications,Volume 273, Issue 3, 2000, Pages 1063-1068, ISSN 0006-291X, https://doi.org/10.1006/bbrc.2000.3071
4. Bhattacharyya AK, Connor WE. Beta-sitosterolemia and xanthomatosis. A newly described lipid storage disease in two sisters. J Clin Invest. 1974 Apr;53(4):1033-43. doi: 10.1172/JCI107640. PMID: 4360855; PMCID: PMC333088.
5. Wang, Z., Cao, L., Su, Y., Wang, G., Wang, R., Yu, Z., Bai, X., & Ruan, C. (2014). Specific macrothrombocytopenia/hemolytic anemia associated with sitosterolemia. *American journal of hematology*, *89*(3), 320–324. https://doi.org/10.1002/ajh.23619
6. Higgins, C., Linton, K. The ATP switch model for ABC transporters. *Nat Struct Mol Biol* **11,** 918–926 (2004). https://doi.org/10.1038/nsmb836
7. Rees, D., Johnson, E. & Lewinson, O. ABC transporters: the power to change. *Nat Rev Mol Cell Biol* **10,** 218–227 (2009). https://doi.org/10.1038/nrm2646
8. Musso, G., Gambino, R., & Cassader, M. (2013). Cholesterol metabolism and the pathogenesis of non-alcoholic steatohepatitis. *Progress in lipid research*, *52*(1), 175–191. https://doi.org/10.1016/j.plipres.2012.11.002
9. Brown, M. S., & Goldstein, J. L. (1997). The SREBP pathway: regulation of cholesterol metabolism by proteolysis of a membrane-bound transcription factor. *Cell*, *89*(3), 331–340. https://doi.org/10.1016/s0092-8674(00)80213-5
10. Linton, M. F., Yancey, P. G., Davies, S. S., Jerome, W. G., Linton, E. F., Song, W. L., Doran, A. C., & Vickers, K. C. (2019). The Role of Lipids and Lipoproteins in Atherosclerosis. In K. R. Feingold (Eds.) et. al., *Endotext*. MDText.com, Inc.
11. McDaniel, A. L., Alger, H. M., Sawyer, J. K., Kelley, K. L., Kock, N. D., Brown, J. M., Temel, R. E., & Rudel, L. L. (2013). Phytosterol feeding causes toxicity in ABCG5/G8 knockout mice. *The American journal of pathology*, *182*(4), 1131–1138. https://doi.org/10.1016/j.ajpath.2012.12.014
12. Izar, M. C., Tegani, D. M., Kasmas, S. H., & Fonseca, F. A. (2011). Phytosterols and phytosterolemia: gene-diet interactions. *Genes & nutrition*, *6*(1), 17–26. https://doi.org/10.1007/s12263-010-0182-x

13. Cohn, J. S., Kamili, A., Wat, E., Chung, R. W., & Tandy, S. (2010). Reduction in intestinal cholesterol absorption by various food components: mechanisms and implications. *Atherosclerosis. Supplements*, *11*(1), 45–48. https://doi.org/10.1016/j.atherosclerosissup.2010.04.004

14. Sugano, M., Morioka, H., & Ikeda, I. (1977). A comparison of hypocholesterolemic activity of beta-sitosterol and beta-sitostanol in rats. *The Journal of nutrition*, *107*(11), 2011–2019. https://doi.org/10.1093/jn/107.11.2011

15. Brufau G, Kuipers F, Lin Y, Trautwein EA, Groen AK. A reappraisal of the mechanism by which plant sterols promote neutral sterol loss in mice. PLoS One. 2011;6(6):e21576. doi: 10.1371/journal.pone.0021576. Epub 2011 Jun 30. PMID: 21738715; PMCID: PMC3128081.

16. Wittenburg H, Carey MC. Biliary cholesterol secretion by the twinned sterol half-transporters ABCG5 and ABCG8. J Clin Invest. 2002 Sep;110(5):605-9. doi: 10.1172/JCI16548. PMID: 12208859; PMCID: PMC151117.

17. Kangmo Lu, Mi-Hye Lee, Shailendra B Patel, Dietary cholesterol absorption; more than just bile, Trends in Endocrinology & Metabolism, Volume 12, Issue 7, 2001, Pages 314-320, ISSN 1043-2760, https://doi.org/10.1016/S1043-2760(01)00433-7. (https://www.sciencedirect.com/science/article/pii/S1043276001004337)

18. Davis, H. R., Jr, Zhu, L. J., Hoos, L. M., Tetzloff, G., Maguire, M., Liu, J., Yao, X., Iyer, S. P., Lam, M. H., Lund, E. G., Detmers, P. A., Graziano, M. P., & Altmann, S. W. (2004). Niemann-Pick C1 Like 1 (NPC1L1) is the intestinal phytosterol and cholesterol transporter and a key modulator of whole-body cholesterol homeostasis. *The Journal of biological chemistry*, *279*(32), 33586–33592. https://doi.org/10.1074/jbc.M405817200

19. Altmann, S. W., Davis,Harry R.,,Jr, Li-ji, Z., Yao, X., & al, e. (2004). Niemann-Pick C1 Like 1 Protein Is Critical for Intestinal Cholesterol Absorption. *Science, 303*(5661), 1201-4. http://ezproxy.uky.edu/login?url=https://www.proquest.com/scholarly-journals/niemann-pick-c1-like-1-protein-is-critical/docview/213596845/se-2?accountid=11836

20. Nguyen TM, Sawyer JK, Kelley KL, Davis MA, Rudel LL. Cholesterol esterification by ACAT2 is essential for efficient intestinal cholesterol absorption: evidence from thoracic lymph duct cannulation. J Lipid Res. 2012 Jan;53(1):95-104. doi: 10.1194/jlr.M018820. Epub 2011 Nov 1. PMID: 22045928; PMCID: PMC3243485.

21. Glomset J. A. (1968). The plasma lecithins:cholesterol acyltransferase reaction. *Journal of lipid research*, *9*(2), 155–167.

22. J.A. Glomset, in: G.J. Nelson (Ed.), Plasma Lipids and Lipoproteins, Wiley Interscience, New York, 1972, pp. 745–787.

23. Krieger M. Charting the fate of the "good cholesterol": identification and characterization of the high-density lipoprotein receptor SR-BI. *Annu. Rev. Biochem.* **68**, 523–558 (1999).

24. Gerloff, T., Stieger, B., Hagenbuch, B., Madon, J., Landmann, L., Roth, J., Hofmann, A. F., & Meier, P. J. (1998). The sister of P-glycoprotein represents the

canalicular bile salt export pump of mammalian liver. *The Journal of biological chemistry*, *273*(16), 10046–10050.

25. Bosner MS, Lange LG, Stenson WF, Ostlund RE. Percent cholesterol absorption in normal women and men quantified with dual stable isotopic tracers and negative ion mass spectrometry. *J Lipid Res.* 1999 Feb;40(2):302–8.

26. Dawson PA. Role of the intestinal bile acid transporters in bile acid and drug disposition. *Handb Exp Pharmacol.* 2011;201:169–203.

27. van der Velde, A. E., Vrins, C. L., van den Oever, K., Seemann, I., Oude Elferink, R. P., van Eck, M., Kuipers, F., & Groen, A. K. (2008). Regulation of direct transintestinal cholesterol excretion in mice. *American journal of physiology. Gastrointestinal and liver physiology*, *295*(1), G203–G208. https://doi.org/10.1152/ajpgi.90231.2008

28. Grefhorst, A., Verkade, H. J., & Groen, A. K. (2019). The TICE Pathway: Mechanisms and Lipid-Lowering Therapies. *Methodist DeBakey cardiovascular journal*, *15*(1), 70–76. https://doi.org/10.14797/mdcj-15-1-70

29. van der Velde, A. E., Vrins, C. L., van den Oever, K., Kunne, C., Oude Elferink, R. P., Kuipers, F., & Groen, A. K. (2007). Direct intestinal cholesterol secretion contributes significantly to total fecal neutral sterol excretion in mice. *Gastroenterology*, *133*(3), 967–975. https://doi.org/10.1053/j.gastro.2007.06.019

30. Berge, K. E., Tian, H., Graf, G. A., Yu, L., Grishin, N. V., Schultz, J., Kwiterovich, P., Shan, B., Barnes, R., & Hobbs, H. H. (2000). Accumulation of dietary cholesterol in sitosterolemia caused by mutations in adjacent ABC transporters. *Science (New York, N.Y.)*, *290*(5497), 1771–1775. https://doi.org/10.1126/science.290.5497.1771

31. Graf, G. A., Yu, L., Li, W. P., Gerard, R., Tuma, P. L., Cohen, J. C., & Hobbs, H. H. (2003). ABCG5 and ABCG8 are obligate heterodimers for protein trafficking and biliary cholesterol excretion. *The Journal of biological chemistry*, *278*(48), 48275–48282. https://doi.org/10.1074/jbc.M310223200

32. Tsubakio-Yamamoto, K., Nishida, M., Nakagawa-Toyama, Y., Masuda, D., Ohama, T., & Yamashita, S. (2010). Current therapy for patients with sitosterolemia--effect of ezetimibe on plant sterol metabolism. *Journal of atherosclerosis and thrombosis*, *17*(9), 891–900. https://doi.org/10.5551/jat.4614

33. Yoo E. G. (2016). Sitosterolemia: a review and update of pathophysiology, clinical spectrum, diagnosis, and management. *Annals of pediatric endocrinology & metabolism*, *21*(1), 7–14. https://doi.org/10.6065/apem.2016.21.1.7

34. Veit, L., Allegri Machado, G., Bürer, C., Speer, O., & Häberle, J. (2019). Sitosterolemia-10 years observation in two sisters. *JIMD reports*, *48*(1), 4–10. https://doi.org/10.1002/jmd2.12038

35. Hong C, Tontonoz P. 2014. Liver X receptors in lipid metabolism: opportunities for drug discovery. *Nat Rev Drug Discov* 13:433–444. doi: 10.1038/nrd4280.

36. Chen W, Chen G, Head DL, Mangelsdorf DJ, Russell DW. Enzymatic reduction of oxysterols impairs LXR signaling in cultured cells and the livers of mice. Cell Metab. 2007 Jan;5(1):73-9. doi: 10.1016/j.cmet.2006.11.012. PMID: 17189208; PMCID: PMC3080013

37. Repa, J. J., Berge, K. E., Pomajzl, C., Richardson, J. A., Hobbs, H., & Mangelsdorf, D. J. (2002). Regulation of ATP-binding cassette sterol transporters ABCG5 and ABCG8 by the liver X receptors alpha and beta. *The Journal of biological chemistry*, *277*(21), 18793–18800. https://doi.org/10.1074/jbc.M109927200

38. Freeman, L.A., et al., The orphan nuclear receptor LRH-1 activates the ABCG5/ABCG8 intergenic promoter. J Lipid Res, 2004.

39. Sumi, K., et al., Cooperative Interaction between Hepatocyte Nuclear Factor 4{alpha} and GATA Transcription Factors Regulates ATP-Binding Cassette Sterol Transporters ABCG5 and ABCG8. Mol Cell Biol, 2007. 27(12): p. 4248-60.

40. Graf, G. A., Li, W. P., Gerard, R. D., Gelissen, I., White, A., Cohen, J. C., & Hobbs, H. H. (2002). Coexpression of ATP-binding cassette proteins ABCG5 and ABCG8 permits their transport to the apical surface. *The Journal of clinical investigation*, *110*(5), 659–669. https://doi.org/10.1172/JCI16000

41. Wang, J., Mitsche, M. A., Lütjohann, D., Cohen, J. C., Xie, X. S., & Hobbs, H. H. (2015). Relative roles of ABCG5/ABCG8 in liver and intestine. *Journal of lipid research*, *56*(2), 319–330. https://doi.org/10.1194/jlr.M054544

42. Moitra, K., & Dean, M. (2011). Evolution of ABC transporters by gene duplication and their role in human disease. *Biological chemistry*, *392*(1-2), 29–37. https://doi.org/10.1515/BC.2011.006

43. Locher K. P. (2009). Review. Structure and mechanism of ATP-binding cassette transporters. *Philosophical transactions of the Royal Society of London. Series B, Biological sciences*, *364*(1514), 239–245. https://doi.org/10.1098/rstb.2008.0125

44. Procko, E., O'Mara, M. L., Bennett, W. F., Tieleman, D. P., & Gaudet, R. (2009). The mechanism of ABC transporters: general lessons from structural and functional studies of an antigenic peptide transporter. *FASEB journal : official publication of the Federation of American Societies for Experimental Biology*, *23*(5), 1287–1302. https://doi.org/10.1096/fj.08-121855

45. Xiong, J., Feng, J., Yuan, D. *et al.* Tracing the structural evolution of eukaryotic ATP binding cassette transporter superfamily. *Sci Rep* **5,** 16724 (2015). https://doi.org/10.1038/srep16724

46. Online Mendelian Inheritance in Man, OMIM®. McKusick-Nathans Institute of Genetic Medicine, Johns Hopkins University (Baltimore, MD), {Apr. 6, 2022}. World Wide Web URL: https://omim.org/

47. Velamakanni, S., Wei, S. L., Janvilisri, T., & van Veen, H. W. (2007). ABCG transporters: structure, substrate specificities and physiological roles : a brief overview. *Journal of bioenergetics and biomembranes*, *39*(5-6), 465–471. https://doi.org/10.1007/s10863-007-9122-x

48. Cserepes, J., Szentpétery, Z., Seres, L., Ozvegy-Laczka, C., Langmann, T., Schmitz, G., Glavinas, H., Klein, I., Homolya, L., Váradi, A., Sarkadi, B., & Elkind, N. B. (2004). Functional expression and characterization of the human ABCG1 and ABCG4 proteins: indications for heterodimerization. *Biochemical and biophysical research communications*, *320*(3), 860–867. https://doi.org/10.1016/j.bbrc.2004.06.037

49. Lee, JY., Kinch, L., Borek, D. *et al.* Crystal structure of the human sterol transporter ABCG5/ABCG8. *Nature* **533,** 561–564 (2016). https://doi.org/10.1038/nature17666

50. Welsh, M. J., & Smith, A. E. (1993). Molecular mechanisms of CFTR chloride channel dysfunction in cystic fibrosis. *Cell*, *73*(7), 1251–1254. https://doi.org/10.1016/0092-8674(93)90353-r

51. Delaunay, J. L., Durand-Schneider, A. M., Dossier, C., Falguières, T., Gautherot, J., Davit-Spraul, A., Aït-Slimane, T., Housset, C., Jacquemin, E., & Maurice, M. (2016). A functional classification of ABCB4 variations causing progressive familial intrahepatic cholestasis type 3. *Hepatology (Baltimore, Md.)*, *63*(5), 1620–1631. https://doi.org/10.1002/hep.28300

52. Williams K, Segard A, Graf GA. Sitosterolemia: Twenty Years of Discovery of the Function of ABCG5ABCG8. *International Journal of Molecular Sciences,* 2021; 22(5): 2641.

53. Balch, W. E., Morimoto, R. I., Dillin, A., & Kelly, J. W. (2008). Adapting Proteostasis for Disease Intervention. *Science*, *319*(5865), 916–919. http://www.jstor.org/stable/20053369

54. Powers, E. T., Morimoto, R. I., Dillin, A., Kelly, J. W., & Balch, W. E. (2009). Biological and chemical approaches to diseases of proteostasis deficiency. *Annual review of biochemistry*, *78*, 959–991. https://doi.org/10.1146/annurev.biochem.052308.114844

55. Rao, R. V., & Bredesen, D. E. (2004). Misfolded proteins, endoplasmic reticulum stress and neurodegeneration. *Current opinion in cell biology*, *16*(6), 653–662. https://doi.org/10.1016/j.ceb.2004.09.012

56. Bernales, S., Papa, F. R., & Walter, P. (2006). Intracellular signaling by the unfolded protein response. *Annual review of cell and developmental biology*, *22*, 487–508. https://doi.org/10.1146/annurev.cellbio.21.122303.120200

57. McCracken, A. A., & Brodsky, J. L. (1996). Assembly of ER-associated protein degradation in vitro: dependence on cytosol, calnexin, and ATP. *The Journal of cell biology*, *132*(3), 291–298. https://doi.org/10.1083/jcb.132.3.291

58. Vembar, S., Brodsky, J. One step at a time: endoplasmic reticulum-associated degradation. *Nat Rev Mol Cell Biol* **9,** 944–957 (2008). https://doi.org/10.1038/nrm2546

59. Taylor, S. L., Kinchington, P. R., Brooks, A., & Moffat, J. F. (2004). Roscovitine, a cyclin-dependent kinase inhibitor, prevents replication of varicella-zoster virus. *Journal of virology*, *78*(6), 2853–2862. https://doi.org/10.1128/jvi.78.6.2853-2862.2004

60. Norez, C., Vandebrouck, C., Bertrand, J., Noel, S., Durieu, E., Oumata, N., Galons, H., Antigny, F., Chatelier, A., Bois, P., Meijer, L., & Becq, F. (2014). Roscovitine is a proteostasis regulator that corrects the trafficking defect of F508del-CFTR by a CDK-independent mechanism. *British journal of pharmacology*, *171*(21), 4831–4849. https://doi.org/10.1111/bph.12859

61. Vauthier, V., Ben Saad, A., Elie, J. *et al.* Structural analogues of roscovitine rescue the intracellular traffic and the function of ER-retained ABCB4 variants in cell models. *Sci Rep* **9,** 6653 (2019). https://doi.org/10.1038/s41598-019-43111-y

62. Tang, X. X., Ostedgaard, L. S., Hoegger, M. J., Moninger, T. O., Karp, P. H., McMenimen, J. D., Choudhury, B., Varki, A., Stoltz, D. A., & Welsh, M. J. (2016). Acidic pH increases airway surface liquid viscosity in cystic fibrosis. *The Journal of clinical investigation*, *126*(3), 879–891. https://doi.org/10.1172/JCI83922

63. Naehrig, S., Chao, C. M., & Naehrlich, L. (2017). Cystic Fibrosis. *Deutsches Arzteblatt international*, *114*(33-34), 564–574. https://doi.org/10.3238/arztebl.2017.0564

64. Bear, C. E., Li, C. H., Kartner, N., Bridges, R. J., Jensen, T. J., Ramjeesingh, M., & Riordan, J. R. (1992). Purification and functional reconstitution of the cystic fibrosis transmembrane conductance regulator (CFTR). *Cell*, *68*(4), 809–818. https://doi.org/10.1016/0092-8674(92)90155-6

65. Condren, M. E., & Bradshaw, M. D. (2013). Ivacaftor: a novel gene-based therapeutic approach for cystic fibrosis. *The journal of pediatric pharmacology and therapeutics : JPPT : the official journal of PPAG*, *18*(1), 8–13. https://doi.org/10.5863/1551-6776-18.1.8

66. Eckford, P. D., Li, C., Ramjeesingh, M., & Bear, C. E. (2012). Cystic fibrosis transmembrane conductance regulator (CFTR) potentiator VX-770 (ivacaftor) opens the defective channel gate of mutant CFTR in a phosphorylation-dependent but ATP-independent manner. *The Journal of biological chemistry*, *287*(44), 36639–36649. https://doi.org/10.1074/jbc.M112.393637

67. Fohner, A. E., McDonagh, E. M., Clancy, J. P., Whirl Carrillo, M., Altman, R. B., & Klein, T. E. (2017). PharmGKB summary: ivacaftor pathway, pharmacokinetics/pharmacodynamics. *Pharmacogenetics and genomics*, *27*(1), 39–42. https://doi.org/10.1097/FPC.0000000000000246

68. Fiedorczuk, K., & Chen, J. (2022). Mechanism of CFTR correction by type I folding correctors. *Cell*, *185*(1), 158–168.e11. https://doi.org/10.1016/j.cell.2021.12.009

69. Woodward, O. M., Tukaye, D. N., Cui, J., Greenwell, P., Constantoulakis, L. M., Parker, B. S., Rao, A., Köttgen, M., Maloney, P. C., & Guggino, W. B. (2013). Gout-causing Q141K mutation in ABCG2 leads to instability of the nucleotide-binding domain and can be corrected with small molecules. *Proceedings of the National Academy of Sciences of the United States of America*, *110*(13), 5223–5228. https://doi.org/10.1073/pnas.1214530110

70. Wang, T., Larcher, L. M., Ma, L., & Veedu, R. N. (2018). Systematic Screening of Commonly Used Commercial Transfection Reagents towards Efficient Transfection of Single-Stranded Oligonucleotides. *Molecules (Basel, Switzerland)*, *23*(10), 2564. https://doi.org/10.3390/molecules23102564

71. Hwang, T. C., & Kirk, K. L. (2013). The CFTR ion channel: gating, regulation, and anion permeation. *Cold Spring Harbor perspectives in medicine*, *3*(1), a009498. https://doi.org/10.1101/cshperspect.a009498

72. Soutar, A. K., & Naoumova, R. P. (2007). Mechanisms of disease: genetic causes of familial hypercholesterolemia. *Nature clinical practice. Cardiovascular medicine*, *4*(4), 214–225. https://doi.org/10.1038/ncpcardio0836

73. Taylor, N., Manolaridis, I., Jackson, S. M., Kowal, J., Stahlberg, H., & Locher, K. P. (2017). Structure of the human multidrug transporter ABCG2. *Nature*, *546*(7659), 504–509. https://doi.org/10.1038/nature22345

74. Higgins, C., Hiles, I., Salmond, G. *et al.* A family of related ATP-binding subunits coupled to many distinct biological processes in bacteria. *Nature* **323,** 448–450 (1986). https://doi.org/10.1038/323448a0

75. Cuperus, F. J., Claudel, T., Gautherot, J., Halilbasic, E., & Trauner, M. (2014). The role of canalicular ABC transporters in cholestasis. *Drug metabolism and disposition: the biological fate of chemicals*, *42*(4), 546–560. https://doi.org/10.1124/dmd.113.056358

76. Nam, S. M., & Jeon, Y. J. (2019). Proteostasis In The Endoplasmic Reticulum: Road to Cure. *Cancers*, *11*(11), 1793. https://doi.org/10.3390/cancers11111793

77. Lippincott-Schwartz, J., Bonifacino, J. S., Yuan, L. C., & Klausner, R. D. (1988). Degradation from the endoplasmic reticulum: disposing of newly synthesized proteins. *Cell*, *54*(2), 209–220. https://doi.org/10.1016/0092-8674(88)90553-3

78. Van Goor F, Hadida S, Grootenhuis PD, et al. Rescue of CF airway epithelial cell function in vitro by a CFTR potentiator, VX-770. *Proc Natl Acad Sci U S A*. 2009;106(44):18825-18830. doi:10.1073/pnas.0904709106

79. Bianchi TS and Bauer JE (2011) Particulate Organic Carbon Cycling and Transformation. In: Wolanski E and McLusky DS (eds.) Treatise on Estuarine and Coastal Science, Vol 5, pp. 69–117. Waltham: Academic Press.

80. Lu, K., Lee, M. H., & Patel, S. B. (2001). Dietary cholesterol absorption; more than just bile. *Trends in endocrinology and metabolism: TEM*, *12*(7), 314–320. https://doi.org/10.1016/s1043-2760(01)00433-7

81. Norlin, M., & Wikvall, K. (2007). Enzymes in the conversion of cholesterol into bile acids. *Current molecular medicine*, *7*(2), 199–218. https://doi.org/10.2174/156652407780059168

82. Stefková, J., Poledne, R., & Hubácek, J. A. (2004). ATP-binding cassette (ABC) transporters in human metabolism and diseases. *Physiological research*, *53*(3), 235–243.

83. Procko, E., Ferrin-O'Connell, I., Ng, S. L., & Gaudet, R. (2006). Distinct structural and functional properties of the ATPase sites in an asymmetric ABC transporter. *Molecular cell*, *24*(1), 51–62. https://doi.org/10.1016/j.molcel.2006.07.034

84. Kusuhara, H., & Sugiyama, Y. (2007). ATP-binding cassette, subfamily G (ABCG family). *Pflugers Archiv : European journal of physiology*, *453*(5), 735–744. https://doi.org/10.1007/s00424-006-0134-x

85. Kullak-Ublick, G. A., Stieger, B., & Meier, P. J. (2004). Enterohepatic bile salt transporters in normal physiology and liver disease. *Gastroenterology*, *126*(1), 322–342. https://doi.org/10.1053/j.gastro.2003.06.005

86. Salen, G., Ahrens, E. H., Jr, & Grundy, S. M. (1970). Metabolism of beta-sitosterol in man. *The Journal of clinical investigation*, *49*(5), 952–967. https://doi.org/10.1172/JCI106315

87. Yamamoto, H., Yamanashi, Y., Takada, T., Mu, S., Tanaka, Y., Komine, T., & Suzuki, H. (2019). Hepatic Expression of Niemann-Pick C1-Like 1, a Cholesterol Reabsorber from Bile, Exacerbates Western Diet-Induced Atherosclerosis in LDL

Receptor Mutant Mice. *Molecular pharmacology*, *96*(1), 47–55. https://doi.org/10.1124/mol.119.115840

88. Hazard, S. E., & Patel, S. B. (2007). Sterolins ABCG5 and ABCG8: regulators of whole body dietary sterols. *Pflugers Archiv : European journal of physiology*, *453*(5), 745–752. https://doi.org/10.1007/s00424-005-0040-7

89. Horton, J. D., Shah, N. A., Warrington, J. A., Anderson, N. N., Park, S. W., Brown, M. S., & Goldstein, J. L. (2003). Combined analysis of oligonucleotide microarray data from transgenic and knockout mice identifies direct SREBP target genes. *Proceedings of the National Academy of Sciences of the United States of America*, *100*(21), 12027–12032. https://doi.org/10.1073/pnas.1534923100

90. Venkateswaran, A., Laffitte, B. A., Joseph, S. B., Mak, P. A., Wilpitz, D. C., Edwards, P. A., & Tontonoz, P. (2000). Control of cellular cholesterol efflux by the nuclear oxysterol receptor LXR alpha. *Proceedings of the National Academy of Sciences of the United States of America*, *97*(22), 12097–12102. https://doi.org/10.1073/pnas.200367697

91. Yu, L., Gupta, S., Xu, F., Liverman, A. D., Moschetta, A., Mangelsdorf, D. J., Repa, J. J., Hobbs, H. H., & Cohen, J. C. (2005). Expression of ABCG5 and ABCG8 is required for regulation of biliary cholesterol secretion. *The Journal of biological chemistry*, *280*(10), 8742–8747.

92. Chiang J. Y. (2013). Bile acid metabolism and signaling. *Comprehensive Physiology*, *3*(3), 1191–1212. https://doi.org/10.1002/cphy.c120023

93. Jonas A. (2000). Lecithin cholesterol acyltransferase. *Biochimica et biophysica acta*, *1529*(1-3), 245–256. https://doi.org/10.1016/s1388-1981(00)00153-0

94. Wang J., Grishin N., Kinch L., Cohen J.C., Hobbs H.H. and Xie X.S. (2011) Sequences in the nonconsensus nucleotide-binding domain of ABCG5/ABCG8 required for sterol transport. *J. Biol. Chem.* 286, 7308–7314 10.1074/jbc.M110.210880

95. Altmann, S. W., Davis, H. R., Zhu, L., Yao, X., Hoos, L. M., Tetzloff, G., Sai Prasad N. Iyer, Maguire, M., Golovko, A., Zeng, M., Wang, L., Murgolo, N., & Graziano, M. P. (2004). Niemann-Pick C1 like 1 Protein Is Critical for Intestinal Cholesterol Absorption. *Science*, *303*(5661), 1201–1204. http://www.jstor.org/stable/3836300

96. Xavier, B. M., Zein, A. A., Venes, A., Wang, J., & Lee, J. Y. (2020). Transmembrane Polar Relay Drives the Allosteric Regulation for ABCG5/G8 Sterol Transporter. *International journal of molecular sciences*, *21*(22), 8747. https://doi.org/10.3390/ijms21228747

97. Hunt, J. F., Wang, C., & Ford, R. C. (2013). Cystic fibrosis transmembrane conductance regulator (ABCC7) structure. *Cold Spring Harbor perspectives in medicine*, *3*(2), a009514. https://doi.org/10.1101/cshperspect.a009514

98. Stieger B. (2011). The role of the sodium-taurocholate cotransporting polypeptide (NTCP) and of the bile salt export pump (BSEP) in physiology and pathophysiology of bile formation. *Handbook of experimental pharmacology*, (201), 205–259. https://doi.org/10.1007/978-3-642-14541-4_5

VITA

1. Born in Kalamazoo, MI.
2. Bachelors of Science from the University of South Florida (May 2020), Enrolled at the University of Kentucky Medical Science program.
3. American Heart Association ATVB Travel Grant for Early Career Investigators Recipient (2022)
4. Brittney Poole